



**HAL**  
open science

## Peatland contribution to stream organic carbon exports from a montane watershed

Thomas Rosset, Laure Gandois, Gaël Le Roux, Roman Teisserenc, Pilar  
Durantez, Thierry Camboulive, Stéphane Binet

### ► To cite this version:

Thomas Rosset, Laure Gandois, Gaël Le Roux, Roman Teisserenc, Pilar Durantez, et al.. Peatland contribution to stream organic carbon exports from a montane watershed. *Journal of Geophysical Research: Biogeosciences*, 2019, 124 (11), pp.3448-3464. 10.1029/2019JG005142 . hal-02333554

**HAL Id: hal-02333554**

**<https://hal.science/hal-02333554v1>**

Submitted on 21 Nov 2019

**HAL** is a multi-disciplinary open access archive for the deposit and dissemination of scientific research documents, whether they are published or not. The documents may come from teaching and research institutions in France or abroad, or from public or private research centers.

L'archive ouverte pluridisciplinaire **HAL**, est destinée au dépôt et à la diffusion de documents scientifiques de niveau recherche, publiés ou non, émanant des établissements d'enseignement et de recherche français ou étrangers, des laboratoires publics ou privés.

## JGR Biogeosciences

## RESEARCH ARTICLE

10.1029/2019JG005142

## Key Points:

- High-frequency monitoring revealed that  $46\% \pm 3\%$  of the stream organic carbon exports occurs during high discharge events (9% of time)
- A small peatland area (3%) contributes at least 63% of the stream organic carbon exports from a mountainous watershed
- DOC specific flux from the studied montane peatland ranges from  $16.1 \pm 0.4$  to  $34.6 \pm 1.5$  g C m<sup>-2</sup> year<sup>-1</sup>

## Supporting Information:

- Supporting Information S1

## Correspondence to:

T. Rosset,  
thomas.rosset@ensat.fr

## Citation:

Rosset, T., Gandois, L., Le Roux, G., Teisserenc, R., Durantez Jimenez, P., Camboulive, T., & Binet, S. (2019). Peatland contribution to stream organic carbon exports from a montane watershed. *Journal of Geophysical Research: Biogeosciences*, 124. <https://doi.org/10.1029/2019JG005142>

Received 13 MAR 2019

Accepted 15 AUG 2019

Accepted article online 19 OCT 2019

## Author Contributions:

**Conceptualization:** T. Rosset, L. Gandois, G. Le Roux, R. Teisserenc, S. Binet

**Data curation:** T. Rosset, L. Gandois, S. Binet

**Formal analysis:** T. Rosset, L. Gandois, S. Binet

**Funding acquisition:** L. Gandois, G. Le Roux, S. Binet

**Investigation:** T. Rosset, L. Gandois, G. Le Roux, R. Teisserenc, P. Durantez Jimenez, T. Camboulive, S. Binet

**Methodology:** T. Rosset, L. Gandois, S. Binet

**Project administration:** T. Rosset, L. Gandois, G. Le Roux, S. Binet






**Resources:** T. Rosset, L. Gandois, P. Durantez Jimenez, T. Camboulive, S. Binet

**Software:** T. Rosset, S. Binet

**Supervision:** L. Gandois, G. Le Roux, S. Binet

(continued)

## Peatland Contribution to Stream Organic Carbon Exports From a Montane Watershed

T. Rosset<sup>1,2</sup> , L. Gandois<sup>1</sup> , G. Le Roux<sup>1</sup> , R. Teisserenc<sup>1</sup> , P. Durantez Jimenez<sup>1</sup>, T. Camboulive<sup>1</sup>, and S. Binet<sup>3</sup> 

<sup>1</sup>EcoLab, Université de Toulouse, CNRS, Toulouse, France, <sup>2</sup>LabEx DRIIHM, CNRS/INEE, Toulouse, France, <sup>3</sup>CNRS/INSU, BRGM, ISTO, Université d'Orléans, Orléans, France

**Abstract** Mountains contain many small and fragmented peatlands within watersheds. As they are difficult to monitor, their role in the water and carbon cycle is often disregarded. This study aims to assess the stream organic carbon exports from a montane peatland and characterizes its contribution to the water chemistry in a headstream watershed. High frequency in situ monitoring of turbidity and fDOM were used to quantify respectively particulate organic carbon (POC) and dissolved organic carbon (DOC) exports at the inlet and outlet of a peatland over three years in a French Pyrenean watershed (1,343 m.a.s.l.). The DOC and POC signals are both highly dynamic, characterized by numerous short peaks lasting from a few hours to a few days. Forty-six percent of the exports occurred during 9% of the time corresponding to the highest flows monitored at the outlet. Despite its small area (3%) within the watershed, the peatland contributes at least 63% of the DOC export at the outlet. The specific DOC flux ranges from  $16.1 \pm 0.4$  to  $34.6 \pm 1.5$  g m<sup>2</sup> year<sup>-1</sup>. POC contributes 17% of the total stream organic carbon exports from the watershed. As the frequency of extreme climatic events is expected to increase in the context of climate change, further studies should be conducted to understand the evolution of underestimated mountainous peatland carbon fluxes and their implication in the carbon cycle of headwaters.

**Plain Language Summary** Since the last glacial period, peatlands have accumulated large stocks of organic carbon. Despite representing only 3% of global continental surfaces, they store about 22% of the continental soil carbon stock. In the context of global change, peatland carbon sequestration capacity needs to be carefully monitored. In addition to greenhouse gas exchanges with the atmosphere, determining this capacity requires the quantification of aquatic organic carbon exports. Aquatic organic carbon exports have rarely been investigated at mountainous peatlands. Moreover, global change is expected to drastically modify mountain hydrology, influencing aquatic carbon exports and carbon balance of mountainous peatlands. Using high frequency in situ instrumentation, this study shows the annual quantity of aquatic organic carbon exported from a montane peatland in the French Pyrenees is in the same range as Northern lowland peatlands. These highly variable exports mainly occur during high discharge events due to snowmelt or rainfalls. Despite its restricted area, this montane peatland is the main contributor of aquatic organic carbon in the watershed. Peatlands influence headwater chemistry and further study must be conducted to monitor the evolution of these mountainous carbon stocks.

## 1. Introduction

Mountains represent around 25% of the global continental surfaces excluding Greenland and Antarctica (Kapos et al., 2000; Meybeck et al., 2001). They play a key role in the global water cycle by storing and supplying fresh water to lowlands (Viviroli et al., 2007). Thanks to these high-altitude water storages, peatlands have been able to form in many mountainous regions over the world since (~15,000 years BP) the last ice age (Chen et al., 2014; Chimner & Cooper, 2003; Cubizolle & Thebaud, 2014; Dodson, 1987; Dudová et al., 2013; Squeo et al., 2006). The surface coverage of mountainous peatlands (>1,000 m.a.s.l.) is strongly controlled by topography (Chimner et al., 2010), and consequently, they are never mentioned in global carbon assessments (Leifeld & Menichetti, 2018; Scharlemann et al., 2014; Yu et al., 2010). Although taken individually their size is negligible compared to vast high latitude or tropical peatlands, they store between ~1,200 (Cooper et al., 2012) and ~1,500 Mg C ha<sup>-1</sup> (Hribljan et al., 2015), which concurs with the average storage of 1,330 Mg C ha<sup>-1</sup> defined for boreal peatlands (Gorham, 1991). Summed together mountainous

**Validation:** T. Rosset, L. Gandois, S. Binet

**Visualization:** T. Rosset

**Writing - original draft:** T. Rosset, L. Gandois, S. Binet

**Writing - review & editing:** T. Rosset, L. Gandois, G. Le Roux, R. Teisserenc, P. Durantez Jimenez, S. Binet

peatlands may represent a valuable carbon stock that needs to be defined globally, understood (Morris et al., 2018) and preserved through current global changes. Because of their remote location, peatlands in mountains are much less studied than their lowland counterparts and only a few studies have investigated their carbon dynamics. These studies mainly focused on gaseous carbon fluxes (Chimner & Cooper, 2003; Pullens et al., 2016) or carbon stock accumulation (Chen et al., 2014; Drexler et al., 2015), but only one mountainous site in Germany has been investigated with regard to stream organic carbon exports (Birkel et al., 2017; Broder & Biester, 2015).

The stream exports of carbon from peatlands have attracted scientific interest over the last decades (Cole et al., 2007; Gandois et al., 2013; Laudon et al., 2011; Roulet & Moore, 2006; Webb et al., 2018). Due to their high organic carbon content and hydraulic connectivity to streams, peatlands have been identified as major carbon contributors to surface waters, both globally (Aitkenhead & McDowell, 2000; Hope et al., 1994) and locally (Ågren et al., 2014; Billett et al., 2006; Laudon et al., 2011). Stream carbon exports include dissolved organic carbon (DOC) and particulate organic carbon (POC) as well as dissolved CO<sub>2</sub> and CH<sub>4</sub> (Webb et al., 2018). In vast and peat-dominated watersheds, DOC is the main form, contributing more than 90% of total carbon exports (Dinsmore et al., 2010; Hope et al., 2001; Laudon et al., 2011; Leach et al., 2016; Roulet et al., 2007). These exports have been shown to be crucial in establishing the net carbon balance of peatlands (Dinsmore et al., 2010; Nilsson et al., 2008), as they may exceed the Net Ecosystem carbon Exchange (Roulet et al., 2007). In addition to playing an important role in the peatland carbon cycle (Holden, 2005), exports of stream organic matter from peatlands have several implications: they can disrupt the downstream food chain and impact the biomass production (Carpenter & Pace, 1997), they can affect the quality of drinking water (Ritson, 2015; R. Tang et al., 2013), they can transport potentially harmful elements along inland waters (Broder & Biester, 2017; Rothwell et al., 2007; Tipping et al., 2003), and they can become a considerable source of atmospheric CO<sub>2</sub> after being mineralized through inland waters (Dawson et al., 2004; Dean et al., 2019; Moody et al., 2013).

Stream organic carbon exports (DOC and POC) from lowland peatlands present clear seasonal and interannual variability related to meteorological and hydrological conditions (Dinsmore et al., 2013; Leach et al., 2016). This variability is enhanced in alpine or montane altitudinal belts (Holdridge, 1967) where peatlands face extreme weather conditions (storms, flash floods, and large ranges of temperature). However, their remote locations and the unpredictability of sudden climatic events make a relevant water sampling monitoring difficult. Optical properties of the organic matter (absorbance and fluorescence) have been used to develop sensors for high frequency in situ sensing of organic carbon in streams (Downing et al., 2009; Rode et al., 2016). These sensors have revealed unexpected temporal variability for organic carbon concentrations in streams draining peatlands (Austnes, 2010; Grayson & Holden, 2012; Koehler et al., 2009; Pellerin et al., 2011; Ryder et al., 2014; Strohmeier et al., 2013; Tunaley et al., 2016). Associated with high-frequency meteorological and hydrological surveys, stream organic carbon concentration monitoring contributes to a better understanding of the carbon mobilization processes and temporality in the watersheds (Bernard-Jannin et al., 2018; Birkel et al., 2017). High-frequency sensing of streams is also an effective way to compare and question the relevancy of stream carbon export assessments based on sporadic water samples (Walling & Webb, 1985). The purpose of this study was to assess the stream organic carbon (POC and DOC) exports from a montane peatland (1,343 m.a.s.l) over a 3-year period (January) 2015 to (December) 2017 in the French Pyrenees. A high-frequency stream organic carbon monitoring system was deployed at the inlet and the outlet of the peatland to specifically determine its biogeochemical role in the watershed. The scientific objectives of this study were (1) to quantify the stream organic carbon exports from a montane watershed containing a peatland, (2) to assess the specific contribution from the peatland to the watershed stream organic carbon exports, and (3) to characterize stream organic carbon exports drivers and temporality in montane climatic conditions.

## 2. Study Site

The Bernadouze peatland is located at 1,343 m.a.s.l. in the Eastern part of the French Pyrenean mountains (42.80273 N; 1.42361 E). The peatland covers an area of about 4.7 ha and is located in a 1.4 km<sup>2</sup> north exposed and particularly steep watershed (peak Mont Ceint = 2,088 m.a.s.l/average slope = 50%). The peatland is classified as a soligenous fen since it depends on a continuous water supply stemming from

precipitation and surficial runoff (Joosten & Clarke, 2002). Due to its size and its altitude, the Bernadouze fen is representative of the peatlands identified in southwestern Europe alpine and montane areas (Joosten et al., 2017; SOeS, 2013). A particularity of the peatland is that it lies on a major tectonic fault separating limestone and granitic bedrock (Ternet et al., 1997). Located mainly on a limestone bedrock, the watershed integrates water losses in karst features. The soils are shallow and classified as Rendic Leptosols (World Reference Base for Soil Resources). The main vegetation in the watershed is a beech forest which extends from the border of the peatland to 1,800 m.a.s.l. The highest areas are covered by grassland, cliffs, and rocks.

From a post glacial lake, the peatland has accumulated over 10,000 years to an average depth of 2 m with extreme accumulation zones of up to 9.5 m (Jalut et al., 1982; Reille, 1990). The current vegetation is typical of a minerotrophic peatland with species such as *Carex demissa* and *Equisetum fluviatile*. However, the presence of small hummocks of *Sphagnum palustre* and *Sphagnum capillifolium* reveals progressive ombrotrophic processes in some peatland areas (Erudel et al., 2017; Henry et al., 2014).

Over the 2015 to 2017 period, the annual precipitations and mean annual temperature of the site were, respectively,  $1,718 \pm 127$  mm year<sup>-1</sup> and  $8.2 \pm 0.6$  °C which concurs with the SAFRAN atmospheric reanalysis over the 1959–2013 period (Vidal et al., 2010) and previous meteorological monitoring in an adjacent valley (Szczypta et al., 2015). The peatland is subject to subzero temperatures and a snow cover from December to April with a snow height exceeding 2 m.

The different subcatchments feeding the peatland were identified from a survey using the Digital Elevation Method with a 5 m horizontal resolution (Marti et al., 2016), and the surfaces of each subcatchment were estimated using the Spatial Analyst-Hydrology-Watershed Toolset in the ARCGIS™ toolbox. In situ flow measurements (section 3.3) showed that the major upstream contributor to the peatland is the subcatchment n°4 (Figure 1). Due to the water losses in karst features, the upstream subcatchment n°2 is not fully hydrologically linked to the outlet which has a variable influence on the discharge at the outlet.

Selective logging was carried out during autumn 2016 in the lowest forested part of subcatchments n°4, 5, and 6.

### 3. Materials and Methods

#### 3.1. Site Instrumentation

Site monitoring started in 2014. This paper presents high-frequency data collected from January 1<sup>st</sup> 2015 to December 31<sup>st</sup> 2017. Precipitation (solid and liquid) and air temperature were recorded every 30 minutes by an automatic weather station installed on a small hill (1416 m.a.s.l.) close to the peatland (Figure 1) (Gascoin & Fanise, 2018).

To identify the specific contribution of the peatland, two identical multiparameter probes (YSI Exo2, USA) were installed at the outlet of the peatland (December 2013) and at inlet n°4 (September 2016). Inlet n°4 is the only perennial stream source flowing through the peatland. At both sites, fluorescence of the dissolved organic matter (fDOM,  $\lambda_{\text{excitation}} = 365 \pm 5$  nm/ $\lambda_{\text{emission}} = 480 \pm 40$  nm), turbidity, water level and temperature, pH, and specific electrical conductance were measured in situ every 30 min. A sensor wiper prevents the sensors from biofouling and the probes were inspected and calibrated monthly.

#### 3.2. Water Sampling and Analysis

Grab water sampling was performed every 2 weeks at inlet n°4 and at the outlet of the peatland. Piezometer wells ([1.5, 2.5]-m depth) (Figure 1), were used to sample porewater on three occasions (2013–2015) during baseflow. Grab water samples were filtered on site using a manual peristaltic pump and 0.22 μm cellulose acetate filters (GSWP04700 Merck-Millipore, USA). To avoid contamination from cellulose, a first batch of collected water was used to rinse the filter before definitive sampling. Water samples were stored in a cool box and brought back to the laboratory where they were stored at 6 °C until analysis. Flood water sampling was performed 4 times at inlet n°4 and 9 times at the outlet using automatic water samplers (ISCO 3700, USA). During each flood, 24 samples of raw water (950 ml) were taken at a frequency based on the observed time lag of discharge (1 hr for rainfall and 4 hr for snowmelt driven flood events). Flood water samples were collected within the 48 hr following the last sampling. Nonpurgeable organic carbon (referred to hereafter as

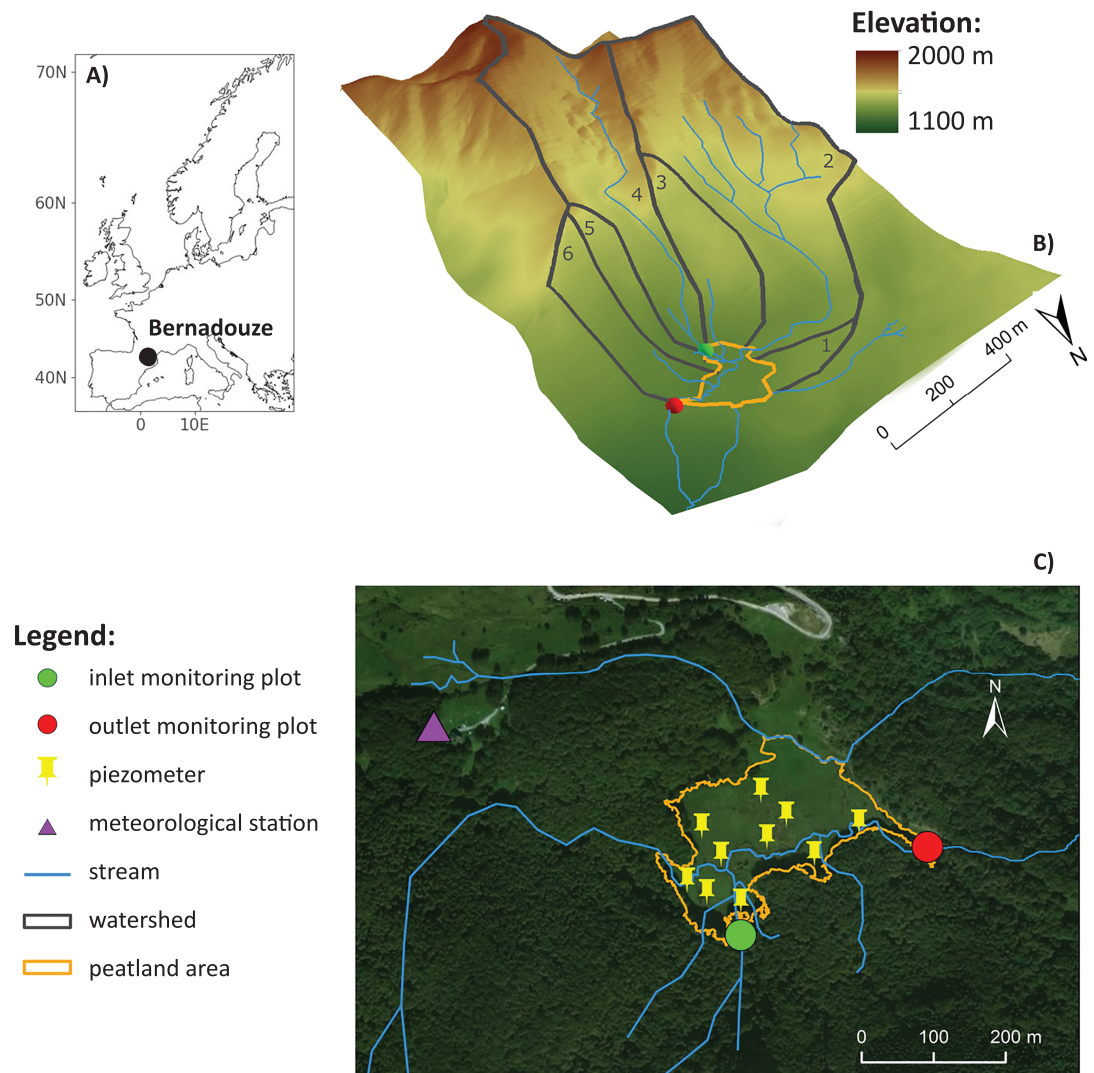


**Figure 1.** (a) Location map of Bernadouze peatland in Europe. (b) Three-dimensional map of the mountainous watershed of Bernadouze peatland. The different subcatchments feeding the peatland are numbered from 1 to 6. Inlet n°4 (green plot) corresponds to the entry of the unique perennial stream flowing across the peatland; it corresponds to the outlet of subcatchment n°4. Due to observed karst discrepancies, subcatchment n°2 does not fully supply the watershed at the outlet of the peatland (red plot). (c) Satellite view of the Bernadouze peatland and the site instrumentation. Map source: Esri, DigitalGlobe, Geoeye, Earthstar Geographics, CNES/Airbus DS, USDA, USGS, AEX, Getmapping, Aerogrid, IGN, IGP, swisstopo, and the GIS User Community.

DOC) concentration was analyzed on filtered samples after acidification to pH 2 with a TOC-5000A analyzer (Shimadzu, Japan). The quantification limit of the analyzer was  $1 \text{ mg l}^{-1}$ . Above this value, the analytical uncertainty was evaluated to  $\pm 0.1 \text{ mg l}^{-1}$ . Reference material included ION-915 and ION96.4 (Environment and Climate Change Canada, Canada). POC concentration of flood samples was estimated by filtering 500 ml of bulk water with a combusted and preweighed  $0.7\text{-}\mu\text{m}$  glass fiber filter (GF/F WHA1825047, Whatman, UK). According to the quantification limit of the weighing scale ( $\pm 0.5 \text{ mg}$ ), only filters containing a suspended material concentration higher than  $1 \text{ mg l}^{-1}$  were considered. Filter areas (disk of 6.5-mm radius) were cut and analyzed with a Flash 2000 Organic Elemental Analyzer (Thermo Fisher Scientific, USA) to determine the POC mass of the considered filter piece. The quantification limit of the analyzer was  $0.200 \mu\text{g}$ . Depending on the homogeneity of the particulates deposited on the filter, between one and 10 replicates were analyzed to assess the POC mass on the whole filter and thus the POC concentration of the sample.

### 3.3. In Situ Data Calibration

Discharge was calculated at 30-min intervals using water levels monitored at inlet n°4 and at the outlet. Two theoretical rating curves were calculated using the xsecAnalyzer tool (NRCS Water Quality and Quantity Technology Development Team, USA) and optimized to fit discharge values acquired by salt dilution measurements (Gees, 1990).

The correction of fDOM data for turbidity, inner filter effect and temperature was explored (de Oliveira et al., 2018; Downing et al., 2012; Watras et al., 2011). Since absorbance values at 254 nm were consistently below 0.6 (de Oliveira et al., 2018), no correction for inner filter effect was applied to the signal. Short peaks of turbidity > 20 FNU potentially disturbed fDOM monitoring (Downing et al., 2012). During these peaks, raw contiguous fDOM data were removed from the data set and linearly interpolated when non disturbed fDOM data were separated by less than 6 hr. No other correction was applied for turbidity. Lastly, fDOM data were corrected for water temperature as mentioned by de Oliveira et al. (2018). High-frequency DOC concentration was calculated using the relationship linking fDOM data to DOC concentration in flood and grab-water samples. The model chosen was a linear regression ( $[DOC] = a \cdot fDOM + b$ ) described by the following parameters ( $a = 0.193$ ,  $b = -0.06$ , number of observations = 167,  $r^2 = 0.93$ ,  $p$  value < 0.001) (supporting information Figure S1). This model was applied at inlet n°4 and at the outlet since fDOM calibration tests had been conducted in the laboratory showing no significant differences between the two sensors. POC concentration at the outlet was estimated at 30-min intervals using a model based on the natural logarithm of the turbidity ( $[POC] = a \cdot \ln(\text{Turbidity}) + b$ ) described by the following parameters ( $a = 0.55$ ,  $b = 0.04$ , number of observations = 30,  $r^2 = 0.65$ ,  $p$  value < 0.01) (supporting information Figure S2). At the inlet, calibration of the turbidity sensor could not be performed because not enough filters contained sufficient material for quantification.

### 3.4. Flood Period Definition and Identification

Flood periods were identified in the discharge signal according to a hydrograph separation method (McDonnell, 2009) specific to the outlet of Bernadouze peatland and compiled in a Python script. In this script, a flood starts with a positive gradient of  $5 \text{ L s}^{-1}$  between two successive sample points, which corresponds to a water elevation of 1 cm at the outlet at low flow. A flood finishes at the end of the subsurface flow compartment on the falling limb of each flood hydrograph. The MRCTools v3.1 software (Posavec et al., 2017) was used to model a master recession curve and define a unique subsurface flow limit specific to the outlet discharge data from 2015 to 2017. To mitigate the high-frequency variability in the discharge signal, it was determined that the end of a flood occurred when the average of four continuous discharge values exceeded the subsurface flow separation limit. Lastly, floods occurring less than 24 hr apart were grouped into a single flood event.

### 3.5. Exports and Specific Flux Calculation

Each of the following equations were written using DOC notation. Equations (1), (5), and (6) are also used for POC.

At each monitoring point  $j$ , the export  $m_{j,DOC}$  was estimated (equation (1)) with  $Q_i$  and  $[DOC]_i$  corresponding to data simultaneously collected at the logging time  $i$  and  $\Delta t$  corresponding to the high-frequency rate of 30 min.

$$m_{j,DOC} = \int (Q \cdot [DOC]) \cdot dt \approx \Delta t \cdot \sum_0^N Q_i \cdot [DOC]_i \quad (1)$$

Based on the subcatchment surface, estimated with the DEM, the specific flux ( $F_j$ ) of each monitoring point is equal to the exported mass divided by the surface ( $A_j$ ) of the subcatchment  $j$  considered:

$$F_{j,DOC} = \frac{m_{j,DOC}}{A_j} \quad (2)$$

From the mass conservation equation, the outlet exported mass can be broken down into different subcatchments:

$$m_{\text{outlet,DOC}} = m_{\text{peatland,DOC}} + \sum_1^6 m_{j,\text{DOC}} \quad (3)$$

Since 2014, stream organic carbon concentrations measured at the outlet of subcatchment n°2 were similar to the ones sampled at the outlet of subcatchment n°4 (supporting information S3). Assuming that subcatchment n°4 is representative of all the six subcatchments that feed the peatland, the specific flux of the peatland can be calculated as follows:

$$F_{\text{peatland,DOC}} = \frac{m_{\text{outlet,DOC}} - \left(\frac{A_{\text{outlet}} - A_{\text{peat}}}{A_{\text{inlet4}}}\right) * m_{\text{inletn}^{\circ}4,\text{DOC}}}{A_{\text{peatland}}} \quad (4)$$

As mentioned previously, the Bernadouze peatland lies on a karst system, which could lead to an overestimation of the feeding area of the outlet due to ground flow loss. Perennial water losses observed along the stream of subcatchment n°2 indicated that this stream does not feed the inlet of the peatland continuously but may occasionally do so during high flow events. These karst discrepancies have an effect on the calculation of specific fluxes because they can reduce the term  $A_{\text{outlet}}$  of the effective catchment area. Therefore, for the rest of the discussion, a specific flux range will be denoted as follows,  $[x,y]$ . The first number ( $x$ ) represents the specific flux calculated with the entire watershed area while the second number ( $y$ ) represents the specific flux calculated after removing the area of subcatchment n°2.

### 3.6. Outliers and Gap Filling

Water level, fDOM, and turbidity outliers due to maintenance were corrected manually by applying linear regressions between the closest validated data. Battery or sensor dysfunctions and wiper failures prevented data acquisition and signal measurements during different periods. A linear model ( $r^2 = 0.99$ ,  $p$  value  $< 0.01$ ) based on total precipitation recorded in Aulus-les-Bains (733 m, (42°48'N, 1°20'E)) was built to generate total daily precipitation in Bernadouze when precipitation data from the in situ weather station were not available. Missing discharge and stream organic carbon concentration (DOC and POC) data were replaced respectively by the extrapolated average (equation (5)) and the discharge weighted average (equation (6)) calculated over the 2015–2017 period. At inlet n°4, annual discharges for 2015 and 2016 were estimated using the precipitation/discharge ratio observed for 2017. Annual DOC exports were estimated with 20% of uncertainty by multiplying the previously estimated annual discharges by the average DOC concentration observed in 2017 at inlet n°4.

$$\bar{Q} = \int_0^t Q(t) * dt \approx \frac{\sum_{i=1}^n Q_i * \Delta t_i}{\sum_{i=1}^n \Delta t_i} \quad (5)$$

with  $\Delta t_i$  = high frequency rate = 30 min

$$\overline{[X]} = \int_0^t [X](t) * Q(t) * dt \approx \frac{\sum_{i=1}^n Q_i * [X]_i * \Delta t_i}{\sum_{i=1}^n Q_i * \Delta t_i} \quad (6)$$

### 3.7. Flux Uncertainties

A Monte Carlo simulation approach was used to estimate uncertainties on calculation of the fluxes (equation (2)) as detailed by Cook et al. (2018). At each logging time, discharge and stream organic carbon concentration values were defined according to a normal distribution centered on the observed data with a standard deviation defined as follows: for discharge data at the outlet, the standard error was set at 7% of the observed data for values lower than  $360 \text{ L s}^{-1}$  and 17% for higher ones; at the inlet, the discharge standard error was set at 10% for all values. The standard errors for both DOC and POC concentration were assumed to be  $\pm 0.5$

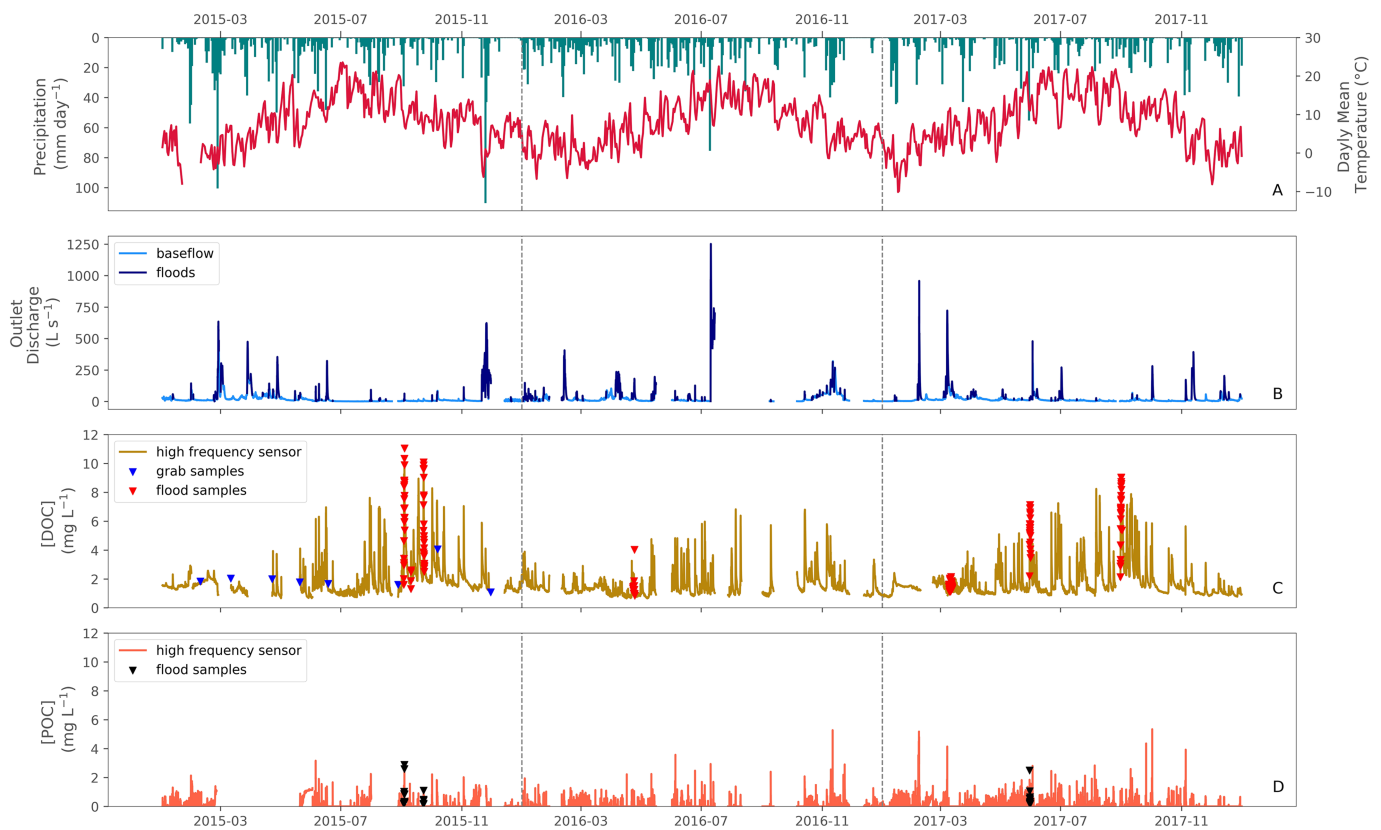


**Figure 2.** Precipitation and air temperature (a), discharge (b), high-frequency DOC concentration (c), and high-frequency POC concentration (d) time series observed at the outlet of the Bernadouze peatland over 3 years (1 January 2015 to 31 December 2017). The vertical grey lines represent a change of year. The dark blue periods on the discharge signal represent floods. Blue and red triangles in timeline (c) refer to DOC concentration measured in grab water samples and automated flood samples respectively. Black triangles in timeline (d) refer to POC concentration measured in automated flood samples.

$\text{mg L}^{-1}$ . After 5,000 iterations for each flux calculation, the best-estimate value was taken as the mean and the standard error estimation was taken as the standard deviation of the flux.

## 4. Results

### 4.1. Outlet Stream Hydrochemistry

At the outlet of Bernadouze peatland, the average baseflow was  $16 \text{ L s}^{-1}$ , ranging from  $0.5$  to  $620 \text{ L s}^{-1}$ . Base flow conditions occurred both during winter (November to February) when most precipitation occurs in the form of snow and during summer (July to September) when evapotranspiration processes are highly active due to high temperatures and less frequent rain events (Figure 2). High flows (flood events) occurred throughout the year and lasted from 90 min to 10 days. They originate from snowmelt (December to April) or heavy rainfall associated with rises in air temperature (May to November). Rain events caused rapid discharge responses ( $\sim 1 \text{ hr}$ ), with sharp discharge gradients (e.g., from  $2$  to  $722 \text{ L s}^{-1}$  in  $1 \text{ hr}$  during the 2016 July flood event). Using the flood definition specified in the method section (3.4), 95 different flood events were identified over three years (dark blue line). They constituted 9% of the timeline and had an average duration of 30 hr. The 95 discharge peaks ranged from  $9$  to  $1251 \text{ L s}^{-1}$ , and the discharge average over those events was  $132 \text{ L s}^{-1}$ .

DOC concentrations ranged from  $0.6$  to  $9.9 \text{ mg L}^{-1}$  at the outlet of Bernadouze peatland, with an average of  $1.5 \text{ mg L}^{-1}$ . The DOC concentration (Figure 2c) presented many short and variable peaks distributed unevenly along the timeline. The largest peak amplitudes occurred each year over periods extending from April to October corresponding to the highest daily mean temperature periods. Each DOC concentration peak started simultaneously with a rising limb in the discharge. However, DOC concentration peaks of



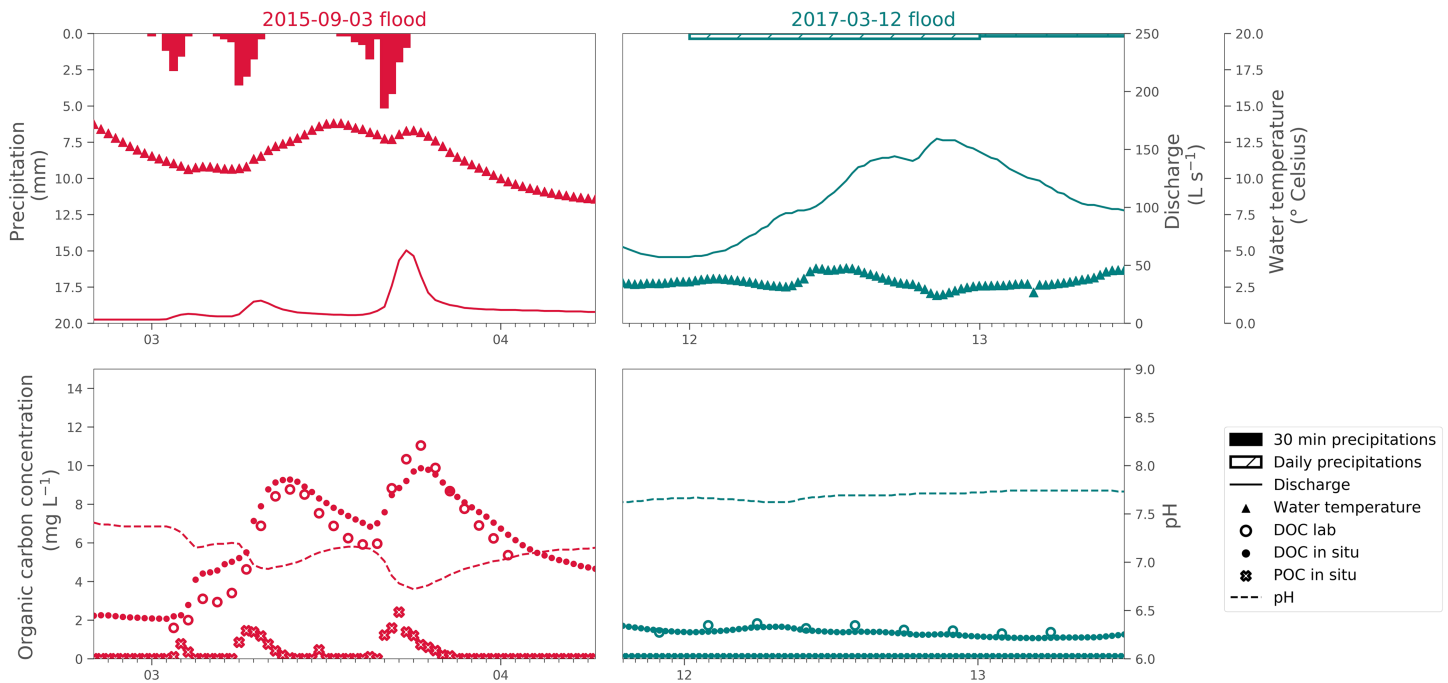


**Figure 3.** High-frequency sampling flood analysis. The summer event (red time series) occurred in September 2015 and the winter event occurred in March 2017. The two top graphs represent precipitation, discharge, and water temperature observed at the outlet of the Bernadouze peatland. Precipitation during the summer event (red) is represented hourly whereas in the second event the rain gauge was damaged. Precipitation was modelled and could only be represented daily. The two bottom graphs represent pH, DOC concentrations derived from fDOM, measured DOC concentrations, and POC concentration derived from turbidity observed at the outlet of the Bernadouze peatland.

similar amplitude were triggered during extremely contrasted discharge events. No systematic relationship was observed between DOC concentration and discharge values.

POC concentration averaged over three years in Bernadouze was  $0.2 \text{ mg L}^{-1}$  and varied between  $0.0$  and  $5.3 \text{ mg L}^{-1}$ . The POC concentration signal (Figure 2d) was composed of low base concentration periods ( $<0.1 \text{ mg L}^{-1}$ ) and intense peaks lasting no longer than 60 min. The POC concentration peaks were distributed throughout the seasons but were more frequent in autumn. Each POC concentration peak started simultaneously with a rising limb in the discharge. However, similar to DOC, no systematic relationship was observed between POC concentration and discharge values. Moreover, no relationship was observed between DOC and POC concentration.

#### 4.2. Detailed Flood Analysis at the Outlet

Figure 3 shows the two seasonal flood patterns monitored and sampled at the outlet of the peatland. Only in situ high-frequency results will be discussed in the following sections. The first flood occurred at the end of the summer of 2015 and was characterized by a maximum DOC concentration of  $9.9 \text{ mg L}^{-1}$ , a maximum POC concentration of  $2.4 \text{ mg L}^{-1}$  and a maximum outflow of  $63 \text{ L s}^{-1}$ . The second flood was monitored at the end of the winter of 2017; it reached a maximum DOC concentration of  $1.8 \text{ mg L}^{-1}$  and a maximum discharge of  $159 \text{ L s}^{-1}$  whereas POC concentration was negligible for the whole period.

During the summer flood (Figure 3a), three precipitation events ( $6 + 10 + 16 = 32 \text{ mm}$ ) generated three successive increases in discharge and organic carbon (DOC and POC) concentration. For each event, organic carbon concentration started to rise simultaneously with discharge. POC concentration peaked simultaneously with discharge whereas DOC concentration peaked 1 hr after the discharge peak. The DOC concentration was not directly related to discharge or precipitation since the second and the third DOC concentration peaks were of similar magnitudes ( $9.3$  and  $9.8 \text{ mg L}^{-1}$ ) for different amounts of rain ( $10$  and  $16 \text{ mm}$ ) and discharge ( $20$  and  $63 \text{ L s}^{-1}$ ) peaks. Water temperature followed a diurnal cycle despite slight decreases observed after the precipitation events. The average water temperature was  $11.5 \text{ }^\circ\text{C}$ , and no

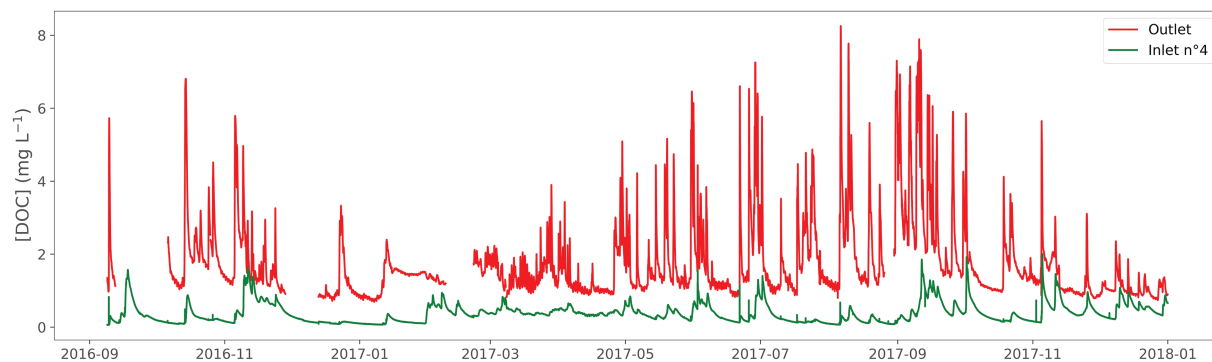


**Figure 4.** DOC concentration time series observed simultaneously at inlet 4 (green) and at the outlet (red) over 16 months (6 September 2016 to 31 December 2017). correlation with other variables was found. DOC and POC exports during this flood were respectively estimated at  $10.4 \pm 0.9$  and  $1.1 \pm 0.6$  kg, with mean export rates of  $226 \pm 21$  g  $30 \text{ min}^{-1}$  and  $16 \pm 9$  g  $30 \text{ min}^{-1}$ .

The winter flood (Figure 3b) was composed of one main discharge elevation due to a small rain event (total over the period = 13 mm). During the discharge event, no organic carbon concentration peaks were observed as the signals remained stable in low ranges from 1.1 to 1.8 mg L<sup>-1</sup> for DOC and were null for POC. The water temperature ranges were low due to the snowmelt [1.9, 3.8] °C with a minimum observed during the highest discharges. DOC exports during this winter flood event were estimated at  $40.5 \pm 15.7$  kg with a mean export rate of  $220 \pm 85$  g  $30 \text{ min}^{-1}$ .

#### 4.3. Inlet and Outlet Hydrochemical Trends

From September 2016 to January 2018 at inlet n°4, DOC concentration ranged from 0.1 to 2.0 mg L<sup>-1</sup> with an average value of 0.6 mg L<sup>-1</sup> (Figure 4). Over the same period at the outlet, DOC concentration ranged from 0.7 to 8.3 mg L<sup>-1</sup> with an average of 1.7 mg L<sup>-1</sup>. Both signals are partitioned between short DOC concentration peak events and long periods of low concentration stabilized around 0.1 mg L<sup>-1</sup> at inlet n°4 and 1.0 mg L<sup>-1</sup> at the outlet. By comparing several DOC concentration peak events in the timeline, it was established that the maximum DOC concentration at the outlet preceded the one at inlet n°4 by an average of 7 hr. When comparing similar events on the timeline, the magnitude ratio of the DOC concentration peaks ( $[\text{DOC outlet}]/[\text{DOC inlet n}^\circ 4]$ ) varied from 1.5 to 21 (adjusted with the 7-hr delay).

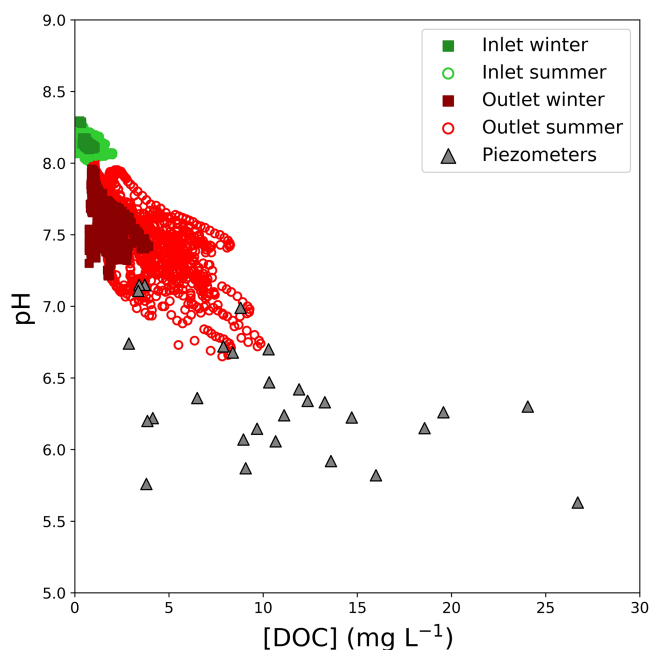


**Figure 5.** DOC concentration versus pH plot representing the 95 flood events observed at the outlet (red plots) and the 41 periods observed simultaneously at the inlet (green plots). Dark colors represent winter flood while light colors represent summer flood. Purple triangles represent DOC concentration measured in different piezometer wells situated within the Bernadouze peatland.

At inlet n°4, pH was stable around 8.1, whatever the hydrological conditions. This was not the case at the outlet where pH ranged between 6.6 and 8.0 (Figure 5). The decreases of pH at the outlet during floods were associated with a rise in DOC concentrations (Figure 5). The outlet water chemistry can be modelled as a mix between two end members: water from Inlet n°4 and peatland porewater observed in the piezometer wells. During flood events, the porewater contribution rose since stream water evolved toward high DOC concentrations ( $>10 \text{ mg L}^{-1}$ ) and lower pH ( $<6.5$ ). This phenomenon was amplified during summer (1 May to 30 November) with ranges 2 times greater than in winter (1 December to 30 April).

#### 4.4. Outlet Stream Organic Carbon Exports

Total exports of organic carbon at the Bernadouze peatland outlet from January 2015 to December 2017 reached  $5,422 \pm 83$  kg with an annual average value of  $1,807 \pm 31$  kg year<sup>-1</sup> (Figure 6). Over that period, the majority of the organic carbon exports occurred in the dissolved form which represented  $83\% \pm 2\%$  of the total export (Figure 6c). Looking at the high-frequency signals, DOC exports at the outlet of Bernadouze

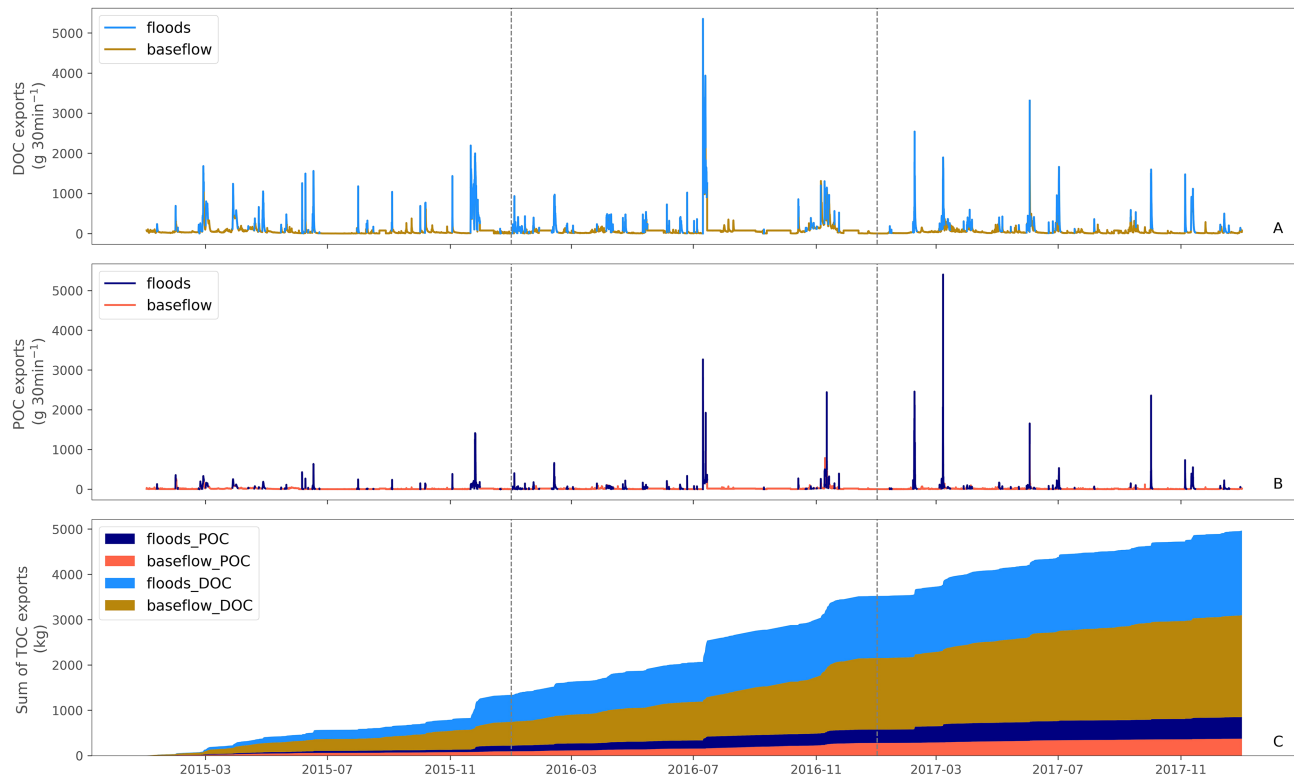


**Figure 6.** DOC exports (a) and POC exports (b) time series and cumulative TOC exports (c) calculated over 3 years in the outlet of Bernadouze peatland. Vertical grey lines represent a change of year. Dark colors represent floods.

watershed ranged from  $0.8 \pm 0.5$  to  $5,352.1 \pm 1,239.9$  g  $30 \text{ min}^{-1}$  with an average value of  $91.6 \pm 28.9$  g  $30 \text{ min}^{-1}$  (Figure 6a) while POC exports ranged from  $0.2 \pm 0.3$  g  $30 \text{ min}^{-1}$  to  $5,403.4 \pm 1,137.2$  g  $30 \text{ min}^{-1}$  with an average value of  $19.1 \pm 18.8$  g  $30 \text{ min}^{-1}$  (Figure 6b). The majority of the high stream carbon exports occurred during floods (blue lines on the high-frequency signals) and this significant flood contribution took the form of sharp increases in the cumulative fluxes (Figure 6c). Over the 3 years of study, flood periods represented  $46\% \pm 3\%$  of the total export of carbon, with a contribution of  $45\% \pm 1\%$  to the total DOC exports and  $54\% \pm 2\%$  of the total POC exports. During baseflow,  $85\% \pm 4\%$  of the stream organic carbon was principally exported in dissolved form at a constant rate of  $55.8 \pm 98.0$  g  $30 \text{ min}^{-1}$ .

#### 4.5. Peatland Contribution to DOC Exports From the Watershed

In 2017, DOC fluxes at inlet n°4 represented 9% of the DOC exports at the outlet (Table 1). Based on a topographical watershed contribution (without water losses in karst), the DOC specific fluxes of inlet n°4 and the entire watershed for 2017 were respectively  $0.3 \pm 0.0$  and  $0.7 \pm 0.0$  g  $\text{m}^2 \text{ year}^{-1}$ . In these conditions, the peatland DOC specific flux reached  $16.1 \pm 0.4$  g  $\text{m}^2 \text{ year}^{-1}$  (equation (4)). Assuming that inlet n°2 is outside the hydrological contribution area (reduced watershed—Table 1), DOC specific flux at the outlet reached  $1.6 \pm 0.0$  g  $\text{m}^2 \text{ year}^{-1}$  and specific flux of the peatland becomes  $21.2 \pm 0.4$  g  $\text{m}^2 \text{ year}^{-1}$ . According to the DOC specific flux difference between the outlet and inlet n°4, the Bernadouze peatland contributed between 64% and 84% of the outlet DOC specific flux. For 2015 and 2016, the peatland DOC specific flux was estimated to reach  $[20.2 \pm 2.8, 26.9 \pm 1.5]$  g  $\text{m}^{-2} \text{ year}^{-1}$  and  $[28.4 \pm 2.8, 34.6 \pm 1.5]$  g  $\text{m}^{-2} \text{ year}^{-1}$ , respectively.

## 5. Discussion

### 5.1. Insights From High-Frequency Monitoring

High-frequency monitoring highlights the highly dynamic regime of stream organic concentrations in the watershed of Bernadouze. Sharp increases in concentrations are recorded within hours in accordance

**Table 1**

*Topographical Description of the Watershed of Bernadouze and 2015 to 2017 Annual Summary of Hydroclimatic Data, Stream Organic Carbon Exports and DOC Specific Fluxes at Inlet n°4 and at the Outlet of the Bernadouze Peatland*

		Unit/Year	2015	2016	2017
Watershed	Total area	m <sup>2</sup>		1,646,760	
	Peatland area			46,678	
	Subcatchment n°2 area			382,485	
	Subcatchment n°4 area			916,371	
	Annual precipitation	mm	1854	1698	1603
	Mean annual temperature	°C	8.5	7.5	8.7
Inlet 4	Discharge	m <sup>3</sup>	186,839 (*) ± 37 368	171,084 (*) ± 34 217	161,544 ± 2,293
	DOC Total exports	g	130,787 (*) ± 26 157	119,759 (*) ± 23 952	98,926 ± 1,667
Outlet	Discharge	m <sup>3</sup>	872,929 ± 12,561	1,147,492 ± 16,507	680,309 ± 9,751
	% flood time	%	8	11	8
	DOC total exports	g	1,491,064 ± 23,458	1,828,705 ± 28,290	1,165,299 ± 17,858
	% DOC during flood		49 ± 2	42 ± 2	42 ± 1
	POC Total exports		306,356 ± 8,328	354,974 ± 8,913	275,982 ± 6,751
	%POC during flood		51 ± 4	48 ± 3	66 ± 4
Peatland DOC specific flux	Entire catchment	g m <sup>-2</sup> year <sup>-1</sup>	20.2 ± 2.8	28.4 ± 2.8	16.1 ± 0.4
	Reduced catchment		26.9 ± 1.5	34.6 ± 1.5	21.2 ± 0.4

*Note.* The symbol (\*) means that the figure has been modelled from the precipitation/discharge ratio observed in 2017 for discharge with 20% of uncertainty and from the multiplication of the mean DOC concentration observed in 2017 and the modelled annual discharge for annual DOC exports at inlet n°4. No POC data were assessed at Inlet n°4 during the whole period. Flood periods percentage was monitored at the outlet of the peatland and represents the total period of flood over one xyear. Peatland specific fluxes depend on the contributing area considered: either the entire catchment or the reduced catchment excluding subcatchment n°2.

with the observations reported in other climatic or topographic contexts (Austnes, 2010; Pellerin et al., 2011; Rode et al., 2016; Saraceno et al., 2009; Tunaley et al., 2018). The coupled monitoring of fDOM, turbidity, and discharge shows that all the stream organic carbon concentration peaks are triggered by a simultaneous discharge elevation. However, stream organic carbon concentration peaks are not proportional to discharge (Figure 3) and other high-frequency parameters such as temperature and water table levels must be included in models to understand their variability (Bernard-Jannin et al., 2018; Binet et al., 2013; Birkel et al., 2017; Tunaley et al., 2018).

During the 3-year monitoring period, the Bernadouze peatland experienced many periods of intense hydrological events (Figure 2). Wind colliding with mountains causes dynamic lifting of moisture laden air to higher altitudes (creating orographic clouds). This process favors precipitation (Houze, 2012; Le Roux et al., 2016), and the steepness of the terrain produces high kinetic energy runoff. Both of these parameters induce a high stream discharge potential and reactivity in the watershed (Jeong et al., 2012). Only karst features (upstream subcatchment n°2) or low temperatures (snow precipitation) are likely to slow down or shift a precipitation event in the discharge signal. In such conditions, in situ high-frequency monitoring is imperative to capture the short and erratic flood events which are crucial in the stream organic carbon exports (Figures 2 and 3). At our study site, flood events represent only 9% of the timeline but account for 46% ± 3% of the total stream organic carbon exports from the watershed. A similar contribution of short hydrological events has been reported in the case of rainfall storms in cool lowland peatlands where 45% (Koehler et al., 2009), 50% (Clark et al., 2007), and between 41% and 57% (Hinton et al., 1997) of the DOC is exported during the 10% of the time corresponding to the highest discharge. This is also consistent with the report by Broder and Biester (2015) from a low elevation (~800 m.a.s.l.) montane peatland in the German Harz Mountains where around 40% of the DOC exports occurred during 10% of the time related to high flows. An equivalent ratio is observed in boreal climates where between 50% and 68% of the TOC are exported from peatlands during the 1-month snowmelt period (Laudon et al., 2004). Montane peatlands, such as the Bernadouze site (Figure 3), combine high discharge events from rainfall, when DOC concentrations increase with discharge (transport limited flood), and snowmelt when DOC concentrations are limited by the discharge level (source limited flood) (Pellerin et al., 2011).

On an annual basis, the benefit of high-frequency monitoring for stream organic carbon export quantification can be questioned. The 2015 to 2017 annual DOC exports based on high-frequency DOC and discharge

(equation (1) and Table 1) were compared to the annual DOC export estimations calculated using method n° 5 from (Walling & Webb, 1985) and completed for uncertainties by Hope et al. (1997). This method is based on high-frequency discharge data and DOC concentrations from the grab stream water samples (Figure 2c). The latter estimations differ between  $-8\% \pm 21\%$  and  $+22\% \pm 23\%$  from the ones using high-resolution DOC concentrations. These discrepancies contrast with observations by Koehler et al. (2009) at the Glencar Bog who reported similar DOC exports whatever the considered grab sampling frequency (daily, weekly, and monthly). In Bernadouze, high-frequency monitoring improved the annual DOC export assessments. The differences observed between the two models may originate from the extreme variability of the DOC concentration at the outlet of the fen, which is much stronger than the one reported from the Glencar bog. High-frequency monitoring helped to detect extremely short (few hours) POC peaks at the beginning of flood events. Quantified over the 3-year period, POC exports account for  $17\% \pm 2\%$  of the TOC exports at the outlet of the Bernadouze peatland. This is a relatively high ratio since typical values range from 0.6% ((Laudon et al., 2011) in boreal peatlands, to 5% (Dinsmore et al., 2010) in a northern temperate peatland and from 2% to 8% (Cook et al., 2018; Moore et al., 2013) in tropical peatlands. Higher POC export ratios from peatland have already been reported in the literature by Pawson et al. (2012) who found a 40% ratio from an eroded blanket peatland in the UK and by Ryder et al. (2014) who reported a similar ratio in a forested peatland using high-frequency monitoring. Both the steepness (50%) of the watershed and the high-frequency monitoring can explain the high POC export ratio observed at the outlet of Bernadouze peatland. First, erosion events may occur when hydrological flows are particularly intense. The kinetic energy of the water flowing from the top of the watershed may impact upper peat layers and extract material from rich organic soils in the watershed (Dykes & Warburton, 2007). Second, the high-frequency monitoring helps to detect the sudden POC concentration event which could have been missed at a low sampling frequency in other export assessments (Figures 2d, 3, and S2). Unfortunately, no POC concentration data were available at inlet n°4 to attribute POC export to a specific landscape element (peatland or upstream subcatchments).

Logging activities could also favor organic matter mobilization from the upstream subcatchments and may explain this high POC export ratio. At the outlet of the peatland, few large pulses in POC export were observed during floods after the logging campaign in winter and spring 2017. Similarly, Ryder et al. (2014) reported few POC concentration spikes at the outlet of the peaty Burrishoole watershed after clear felling operations. However, no significant link could be established with clear-felling operation.

## 5.2. Mountain Peatland Contribution to Watershed Dissolved Organic Carbon Export

In mountains such as the Pyrenees, the proportion of peatland in watersheds is very small (3% in this study) (SOeS, 2013). This explains the low DOC concentration (3-year average of  $1.5 \text{ mg L}^{-1}$ ) and watershed DOC specific fluxes ( $[0.7 \pm 0.0; 1.6 \pm 0.0] \text{ g m}^{-2} \text{ year}^{-1}$  in 2017) observed at the outlet of Bernadouze peatland. These figures are about one order of magnitude lower than those observed in lowland peatlands (Fraser et al., 2001; Hope et al., 1994; Laudon et al., 2004). However, lowland peatlands are generally more extended ( $> \text{km}^2$ ) and principally dominated by peat surfaces, with the proportion in the watershed reaching more than 70% (Leach et al., 2016; Ryder et al., 2014), 85% (Dinsmore et al., 2010), or even more (Koehler et al., 2009; Worrall et al., 2003). Direct comparisons between mountain peatlands and lowland sites (Billett et al., 2010; Nilsson et al., 2008; Roulet et al., 2007) may be biased and systemic approaches (in/out observations) such as those developed in this study and by Olefeldt and Roulet (2014) must be deployed to assess the real contribution of small peatland areas to their watersheds.

In Bernadouze, simultaneous inlet and outlet monitoring revealed that the peatland area is the main source of DOC in the watershed. During floods, the water exported at the outlet of the peatland is more acidic and DOC enriched than the one flowing at inlet n°4 (Figures 4 and 5), coming closer to the peatland porewater composition (piezometer wells). Moreover, the high DOC concentration peaks at the outlet occurred several hours before the low DOC concentration peaks at inlet n°4, confirming that the peatland is the source of DOC in the watershed. Higher DOC concentrations at the outlet result from (1) the transfer of DOC enriched “preevent” porewater previously stored within the peat column (Tetzlaff et al., 2014; Tunaley et al., 2016) and (2) the leaching of subsurface nonsaturated peat by event water (Bernard-Jannin et al., 2018).

Previous studies highlighted the high contribution of peatland and peaty areas, such as riparian zones, to organic carbon export in headwater streams in different contexts (Laudon et al., 2011; Ledesma et al.,

2017; Mzobe et al., 2018; Strohmeier et al., 2013; Tunaley et al., 2016). In a watershed, different landscape elements are characterized by heterogeneous DOC specific fluxes and, therefore, contribute more or less to the whole watershed DOC export, depending on their surface distribution (Ågren et al., 2014; Laudon et al., 2011; Olefeldt & Roulet, 2014). In the watershed of Bernadouze in 2017, DOC specific flux of subcatchment n°4 was  $0.3 \pm 0.0 \text{ g m}^{-2} \text{ year}^{-1}$  while DOC specific flux of the peatland was  $[16.1 \pm 0.4; 21.2 \pm 0.4] \text{ g m}^{-2} \text{ year}^{-1}$  depending on the contribution of subcatchment n°2. The contribution of subcatchment n°2 was restricted to short and intense precipitation events when karstic loss capacity was saturated and runoff occurred. Therefore, the higher DOC specific flux value must be considered with caution since DOC export occurred strongly during intense flood events, potentially enlarging briefly the contributing catchment. With a DOC specific flux at least 54 times higher than the upstream catchments, the Bernadouze peatland contributed between 63% and 84% of the DOC outlet exports in 2017. Moreover, this ratio may be underestimated since DOC in-stream processes such as sorption to sediments or mineralization (Cole et al., 2007; Dawson et al., 2004; J. Tang et al., 2018) were not taken into account in this study leading to conservative outlet DOC export and peatland specific flux assessments.

Considering the estimations for 2015 and 2016, the peatland DOC specific flux ranges from  $16.1 \pm 0.4$  to  $34.6 \pm 1.5 \text{ g m}^{-2} \text{ year}^{-1}$  at Bernadouze (Table 1) with a clear interannual variability. In the literature, the interannual variability of peatland specific fluxes appears to be largely influenced by precipitation (Dinsmore et al., 2013; Leach et al., 2016; Roulet et al., 2007) and by the frequency of extreme hydrological events (Clark et al., 2007), which concurs with this study (Figure 1 and Table 1). Even if it is highly variable, the DOC specific flux observed at Bernadouze falls within the wide range  $[1.1; 48.4] \text{ g m}^{-2} \text{ year}^{-1}$  of DOC specific fluxes reported by (Fraser et al., 2001) for wetlands and forested-wetland catchments and it is within the typical  $[20, 30] \text{ g m}^{-2} \text{ year}^{-1}$  range attributed to northern peatlands by Gorham (1995). This flux is consistent with fluxes recently calculated for peat-dominant watersheds under both temperate and boreal climates. For example, DOC exports from Glencar bog in Ireland are estimated at  $14 \pm 1.5 \text{ g m}^{-2} \text{ year}^{-1}$  (Koehler et al., 2009), Burrishoole watershed DOC exports are  $[9.5, 13.7] \text{ g m}^{-2} \text{ year}^{-1}$  (Ryder et al., 2014) while other British peatland DOC specific fluxes range between 9.4 and  $19.3 \text{ g m}^{-2} \text{ year}^{-1}$  (Billett et al., 2010; Worrall et al., 2003). In boreal areas, Roulet et al. (2007) reported a 6-year average specific flux of  $16.4 \pm 3.4 \text{ g m}^{-2} \text{ year}^{-1}$  in Mer Bleue (Canada) while Leach et al. (2016) estimated a DOC specific flux averaged over 12 years of  $12.2 \pm 3.4 \text{ g m}^{-2} \text{ year}^{-1}$  in Degerö Stormyr (Sweden). Finally, they are also consistent with exports monitored by Broder and Biester (2015) from the montane Odersprung bog with a DOC specific flux reaching  $15.5 \pm 6.7 \text{ g m}^{-2} \text{ year}^{-1}$ . More studies need to be conducted in mountains to assess the influence of elevation on peatland DOC specific fluxes since the Bernadouze peatland (1,343 m.a.s.l.) seems to export more than the lower (800 m.a.s.l.) Odersprung bog. Moreover, mountainous areas are expected to be strongly impacted by climate change in the coming years (Nogués-Bravo et al., 2007; Pachauri & IPCC, 2008), which will certainly affect their stream organic carbon specific fluxes. Increasing temperatures and precipitation changes will cause severe shifts in mountainous hydrological regimes (Beniston, 2006; Eckhardt & Ulbrich, 2003; Gobiet et al., 2014) by reducing snow and ice pack (Barry, 1990; Bosson et al., 2019; Zemp et al., 2006). They will also modify the catchment land cover by enhancing thermophilic plant communities and increasing vegetation in alpine climatic belts (Gottfried et al., 2012; Rogora et al., 2018). Extreme rain events are expected to be more frequent in the Pyrenees (Gao et al., 2006) instigating more flood events. Enhancing the 9% flood event ratio measured in Bernadouze, these events may substantially increase the peatland DOC exports and potentially deplete the peatland carbon stocks held in mountains.

## 6. Conclusion

This study is a unique contribution to the understanding of the carbon cycle in montane peatlands and their associated watersheds. At the outlet of the Bernadouze peatland, 46% of the TOC annual exports occur during 9% of the time which represents the seasonal “hot spots” of high discharge (storm and snowmelt). In this context, high frequency in situ monitoring is imperative to accurately assess stream organic carbon exports since it reveals sudden brief peaks of DOC and POC concentration not related to the discharge levels, but

crucial in the export calculations. In this mountainous watershed, DOC is the dominant form exported but POC constitutes 17% of the TOC annual exports at the outlet. The inlet and outlet monitoring shows that a montane peatland (3% of the watershed area) contributes at least 63% of the DOC exports in the watershed. Even if low DOC concentrations are observed at the outlet ( $1.5 \text{ mg L}^{-1}$  average), the DOC specific flux of this montane peatland ranges from  $16.1 \pm 0.4$  to  $34.6 \pm 1.5 \text{ g m}^{-2} \text{ year}^{-1}$  which is consistent with the DOC specific fluxes measured in Northern lowland peatlands. It confirms that these small, fragmented but numerous mountainous peatlands must be considered when assessing the impacts that their stream organic carbon exports may have on headwater stream chemistry.

#### Acknowledgments

All the carbon analyses were performed at the PAPC platform (EcoLab). The authors wish to thank V. Payré-Suc, F. Julien, and D. Lambrigot for assisting in stream organic carbon concentration analysis; F. De Vleeschouwer and D. Allen for assisting in water sampling; E. Lerigoleur for assisting in map design and data management; S. Gascoin et P. Fanise for providing the meteorological data; D. Galop for assisting in site preparation and communication with local policy maker; and E. Woodcock, S. Allen, and E. Rowley-Jolivet for English language assistance. This scientific work was made possible with the logistical support of the French National Forestry Office and the support of the inhabitants of the Haut-Videssos territory. This work is part of a transdisciplinary research program (OHM Haut Videssos) which collects and studies large socio-ecological data from the Haut-Videssos territory. The authors thank the editors and the reviewers for their constructive comments that improved this article. A description of the specific peatland database is available online at <http://ohmpyr-cat.univ-tlse2.fr/geonetwork/srv/fre/catalog.search#/home> website. The data used in this manuscript are described and available on the Pangaea® data repository at <https://doi.org/10.1594/PANGAEA.899200> website. This project was funded by Observatoire Homme-Milieu Pyrénées Haut-Videssos-LABEX DRIIHM and ANR JCJC TRAM (ANR JCJC 15-CE01-008 TRAM). This project was made possible thanks to the support of the LabEx DRIIHM which financed Thomas Rosset's thesis grant. Additional funds from REPLIM project (Interreg V-A POCTEFA 2014-2020) for equipment and publication fee are acknowledged. Weather data and maintenance of Bernadouze weather station by CESBIO are supported by Observatoire Spatial Régional (CNRS-INSU) and CNES-TOSCA. Bernadouze peatland is a part of the SNO Tourbière referenced in <https://deims.org/> under the label OZCAR-RI PEATLAND Bernadouze - France.

#### References

- Ågren, A. M., Buffam, I., Cooper, D. M., Tiwari, T., Evans, C. D., & Laudon, H. (2014). Can the heterogeneity in stream dissolved organic carbon be explained by contributing landscape elements? *Biogeosciences*, *11*(4), 1199–1213. <https://doi.org/10.5194/bg-11-1199-2014>
- Aitkenhead, J. A., & McDowell, W. H. (2000). Soil C:N ratio as a predictor of annual riverine DOC flux at local and global scales. *Global Biogeochemical Cycles*, *14*(1), 127–138. <https://doi.org/10.1029/1999GB900083>
- Austnes, E. (2010). Effects of storm events on mobilisation of dissolved organic matter (DOM) in a Welsh peatland catchment. *Biogeochemistry*, *99*(1), 157–173. <https://doi.org/10.1007/s10533-009-9399-4>
- Barry, R. G. (1990). Changes in mountain climate and glacio-hydrological responses. *Mountain Research and Development*, *10*(2), 161–170. <https://doi.org/10.2307/3673426>
- Beniston, M. (2006). Mountain weather and climate: A general overview and a focus on climatic change in the Alps. *Hydrobiologia*, *562*(1), 3–16. <https://doi.org/10.1007/s10750-005-1802-0>
- Bernard-Jannin, L., Binet, S., Gogo, S., Leroy, F., Défarge, C., Jozja, N., et al. (2018). Hydrological control of dissolved organic carbon dynamics in a rehabilitated *Sphagnum*-dominated peatland: A water-table based modelling approach. *Hydrology and Earth System Sciences*, *22*(9), 4907–4920. <https://doi.org/https://doi.org/10.5194/hess-22-4907-2018>
- Billett, M. F., Charman, D., Clark, J., Evans, C., Evans, M., Ostle, N., et al. (2010). Carbon balance of UK peatlands: Current state of knowledge and future research challenges. *Climate Research*, *45*, 13–29. <https://doi.org/10.3354/cr00903>
- Billett, M. F., Deacon, C. M., Palmer, S. M., Dawson, J. J. C., & Hope, D. (2006). Connecting organic carbon in stream water and soils in a peatland catchment. *Journal of Geophysical Research*, *111*, G02010. <https://doi.org/10.1029/2005JG000065>
- Binet, S., Gogo, S., & Laggoun-Défarge, F. (2013). A water-table dependent reservoir model to investigate the effect of drought and vascular plant invasion on peatland hydrology. *Journal of Hydrology*, *499*, 132–139. <https://doi.org/10.1016/j.jhydrol.2013.06.035>
- Birkel, C., Broder, T., & Biester, H. (2017). Nonlinear and threshold-dominated runoff generation controls DOC export in a small peat catchment. *Journal of Geophysical Research: Biogeosciences*, *122*, 498–513. <https://doi.org/10.1002/2016JG003621>
- Bosson, J.-B., Huss, M., & Osipova, E. (2019). Disappearing world heritage glaciers as a keystone of nature conservation in a changing climate. *Earth's Future*, *7*(4), 469–479. <https://doi.org/10.1029/2018EF001139>
- Broder, T., & Biester, H. (2015). Hydrologic controls on DOC, As and Pb export from a polluted peatland—The importance of heavy rain events, antecedent moisture conditions and hydrological connectivity. *Biogeosciences*, *12*(15), 4651–4664. <https://doi.org/10.5194/bg-12-4651-2015>
- Broder, T., & Biester, H. (2017). Linking major and trace element concentrations in a headwater stream to DOC release and hydrologic conditions in a bog and peaty riparian zone. *Applied Geochemistry*, *87*, 188–201. <https://doi.org/10.1016/j.apgeochem.2017.11.003>
- Carpenter, S. R., & Pace, M. L. (1997). Dystrophy and Eutrophy in Lake Ecosystems: Implications of Fluctuating Inputs. *Oikos*, *78*(1), 3–14. <https://doi.org/10.2307/3545794>
- Chen, H., Yang, G., Peng, C., Zhang, Y., Zhu, D., Zhu, Q., et al. (2014). The carbon stock of alpine peatlands on the Qinghai-Tibetan Plateau during the Holocene and their future fate. *Quaternary Science Reviews*, *95*, 151–158. <https://doi.org/10.1016/j.quascirev.2014.05.003>
- Chimner, R. A., & Cooper, D. J. (2003). Carbon dynamics of pristine and hydrologically modified fens in the southern Rocky Mountains. *Canadian Journal of Botany*, *81*(5), 477–491. <https://doi.org/10.1139/b03-043>
- Chimner, R. A., Lemly, J. M., & Cooper, D. J. (2010). Mountain fen distribution, types and restoration priorities, San Juan Mountains, Colorado, USA. *Wetlands*, *30*(4), 763–771. <https://doi.org/10.1007/s13157-010-0039-5>
- Clark, J. M., Lane, S. N., Chapman, P. J., & Adamson, J. K. (2007). Export of dissolved organic carbon from an upland peatland during storm events: Implications for flux estimates. *Journal of Hydrology*, *347*(3–4), 438–447. <https://doi.org/10.1016/j.jhydrol.2007.09.030>
- Cole, J. J., Prairie, Y. T., Caraco, N. F., McDowell, W. H., Tranvik, L. J., Striegl, R. G., et al. (2007). Plumbing the global carbon cycle: Integrating inland waters into the terrestrial carbon budget. *Ecosystems*, *10*(1), 172–185. <https://doi.org/10.1007/s10021-006-9013-8>
- Cook, S., Whelan, M. J., Evans, C. D., Gauci, V., Peacock, M., Garnett, M. H., et al. (2018). Fluvial organic carbon fluxes from oil palm plantations on tropical peatland. *Biogeosciences*, *15*(24), 7435–7450. <https://doi.org/10.5194/bg-15-7435-2018>
- Cooper, D. J., Chimner, R. A., & Meritt, D. M. (2012). Western mountain wetlands. In *Wetland Habitats of North America: Ecology and Conservation Concerns* (pp. 313–328). Berkeley: University of California Press. Retrieved from <https://www.ucpress.edu/book/9780520271647/wetland-habitats-of-north-america>
- Cubizolle, H., & Thebaud, G. (2014). A geographical model for the altitudinal zonation of mire types in the uplands of western Europe: The example of Les Monts du Forez in eastern France. *Mires & Peat*, *15*(2), 1–16. [http://mires-and-peat.net/media/map15/map\\_15\\_02.pdf](http://mires-and-peat.net/media/map15/map_15_02.pdf)
- Dawson, J. J. C., Billett, M. F., Hope, D., Palmer, S. M., & Deacon, C. M. (2004). Sources and sinks of aquatic carbon in a peatland stream continuum. *Biogeochemistry*, *70*(1), 71–92. <https://doi.org/10.1023/B:BI0G.000049337.66150.f1>
- de Oliveira, G., Bertone, E., Stewart, R., Awad, J., Holland, A., O'Halloran, K., & Bird, S. (2018). Multi-parameter compensation method for accurate in situ fluorescent dissolved organic matter monitoring and properties characterization. *Water*, *10*(9), 1146. <https://doi.org/10.3390/w10091146>
- Dean, J. F., Garnett, M. H., Spyros, E., & Billett, M. F. (2019). The potential hidden age of dissolved organic carbon exported by peatland streams. *Journal of Geophysical Research: Biogeosciences*, *124*(2), 328–341. <https://doi.org/10.1029/2018JG004650>
- Dinsmore, K. J., Billett, M. F., & Dyson, K. E. (2013). Temperature and precipitation drive temporal variability in aquatic carbon and GHG concentrations and fluxes in a peatland catchment. *Global Change Biology*, *19*(7), 2133–2148. <https://doi.org/10.1111/gcb.12209>

- Dinsmore, K. J., Billett, M. F., Skiba, U. M., Rees, R. M., Drewer, J., & Helfter, C. (2010). Role of the aquatic pathway in the carbon and greenhouse gas budgets of a peatland catchment. *Global Change Biology*, *16*(10), 2750–2762. <https://doi.org/10.1111/j.1365-2486.2009.02119.x>
- Dodson, J. R. (1987). Mire Development and environmental change, Barrington Tops, New South Wales, Australia. *Quaternary Research*, *27*(1), 73–81. [https://doi.org/10.1016/0033-5894\(87\)90050-0](https://doi.org/10.1016/0033-5894(87)90050-0)
- Downing, B. D., Boss, E., Bergamaschi, B. A., Fleck, J. A., Lionberger, M. A., Ganju, N. K., et al. (2009). Quantifying fluxes and characterizing compositional changes of dissolved organic matter in aquatic systems in situ using combined acoustic and optical measurements. *Limnology and Oceanography: Methods*, *7*(1), 119–131. <https://doi.org/10.4319/lom.2009.7.119>
- Downing, B. D., Pellerin, B. A., Bergamaschi, B. A., Saraceno, J. F., & Kraus, T. E. C. (2012). Seeing the light: The effects of particles, dissolved materials, and temperature on in situ measurements of DOM fluorescence in rivers and streams. *Limnology and Oceanography: Methods*, *10*(10), 767–775. <https://doi.org/10.4319/lom.2012.10.767>
- Drexler, J. Z., Fuller, C. C., Orlando, J., & Moore, P. E. (2015). Recent rates of carbon accumulation in montane fens of Yosemite National Park, California, U.S.A. *Arctic, Antarctic, and Alpine Research*, *47*(4), 657–669. <https://doi.org/10.1657/AAAR0015-002>
- Dudová, L., Hájková, P., Buchtová, H., & Opravilová, V. (2013). Formation, succession and landscape history of Central-European summit raised bogs: A multiproxy study from the Hrubý Jeseník Mountains. *The Holocene*, *23*(2), 230–242. <https://doi.org/10.1177/0959683612455540>
- Dykes, A. P., & Warburton, J. (2007). Mass movements in peat: A formal classification scheme. *Geomorphology*, *86*(1), 73–93. <https://doi.org/10.1016/j.geomorph.2006.08.009>
- Eckhardt, K., & Ulbrich, U. (2003). Potential impacts of climate change on groundwater recharge and streamflow in a central European low mountain range. *Journal of Hydrology*, *284*(1), 244–252. <https://doi.org/10.1016/j.jhydrol.2003.08.005>
- Erudel, T., Fabre, S., Briottet, X., & Houet, T. (2017). Classification of peatland vegetation types using in situ hyperspectral measurements. In *2017 IEEE International Geoscience and Remote Sensing Symposium (IGARSS)* (pp. 5713–5716). <https://doi.org/10.1109/IGARSS.2017.8128305>
- Fraser, C. J. D., Roulet, N. T., & Moore, T. R. (2001). Hydrology and dissolved organic carbon biogeochemistry in an ombrotrophic bog. *Hydrological Processes*, *15*(16), 3151–3166. <https://doi.org/10.1002/hyp.322>
- Gandois, L., Cobb, A. R., Hei, I. C., Lim, L. B. L., Salim, K. A., & Harvey, C. F. (2013). Impact of deforestation on solid and dissolved organic matter characteristics of tropical peat forests: implications for carbon release. *Biogeochemistry*, *114*(1–3), 183–199. <https://doi.org/10.1007/s10533-012-9799-8>
- Gao, X., Pal, J. S., & Giorgi, F. (2006). Projected changes in mean and extreme precipitation over the Mediterranean region from a high resolution double nested RCM simulation. *Geophysical Research Letters*, *33*, L03706. <https://doi.org/10.1029/2005GL024954>
- Gascoin, S., & Fanise, P. (2018). Bernadouze meteorological data [Data set]. <https://doi.org/10.6096/DV/UQITZ4>
- Gees, A. (1990). Flow measurement under difficult measuring conditions: Field experience with the salt dilution method. In H. Lang & A. Musy (Eds.), *Hydrology in Mountainous Regions I. Hydrological Measurements; The Water Cycle, IAHS Publ* (Vol. 193, pp. 255–262).
- Gobiet, A., Kotlarski, S., Beniston, M., Heinrich, G., Rajczak, J., & Stoffel, M. (2014). 21st century climate change in the European Alps—A review. *Science of The Total Environment*, *493*, 1138–1151. <https://doi.org/10.1016/j.scitotenv.2013.07.050>
- Gorham, E. (1991). Northern peatlands: Role in the Carbon cycle and probable responses to climatic warming. *Ecological Applications*, *1*(2), 182–195. <https://doi.org/10.2307/1941811>
- Gorham, E. (1995). The biogeochemistry of northern peatlands and its possible responses to global warming. In G. M. Woodwell & F. T. Mackenzie (Eds.), *Biotic Feedbacks in the Global Climate System: Will the Warming Feed the Warming?* (pp. 169–186). Oxford University Press, Inc.
- Gottfried, M., Pauli, H., Futschik, A., Akhalkatsi, M., Barančok, P., Benito Alonso, J. L., et al. (2012). Continent-wide response of mountain vegetation to climate change. *Nature Climate Change*, *2*(2), 111–115. <https://doi.org/10.1038/nclimate1329>
- Grayson, R., & Holden, J. (2012). Continuous measurement of spectrophotometric absorbance in peatland streamwater in northern England: Implications for understanding fluvial carbon fluxes. *Hydrological Processes*, *26*(1), 27–39. <https://doi.org/10.1002/hyp.8106>
- Henry, E., Infante Sánchez, M., & Corriol, G. (2014). *Tourbière de Bernadouze (Suc-et-Sentenac, 09). Expérimentation d'une cartographie fine des végétations* (p. 52). Conservatoire botanique national des Pyrénées et de Midi-Pyrénées, Bagnères de Bigorre.
- Hinton, M. J., Schiff, S. L., & English, M. C. (1997). The significance of storms for the concentration and export of dissolved organic carbon from two Precambrian Shield catchments. *Biogeochemistry*, *36*(1), 67–88. <https://doi.org/10.1023/A:1005779711821>
- Holden, J. (2005). Peatland hydrology and carbon release: Why small-scale process matters. *Philosophical Transactions of the Royal Society of London A: Mathematical, Physical and Engineering Sciences*, *363*(1837), 2891–2913. <https://doi.org/10.1098/rsta.2005.1671>
- Holdridge, L. R. (1967). Life zone ecology. *Life Zone Ecology*. (rev. ed.). Retrieved from <https://www.cabdirect.org/cabdirect/abstract/19670604180>
- Hope, D., Billett, M. F., & Cresser, M. S. (1994). A review of the export of carbon in river water: Fluxes and processes. *Environmental Pollution*, *84*(3), 301–324.
- Hope, D., Billett, M. F., & Cresser, M. S. (1997). Exports of organic carbon in two river systems in NE Scotland. *Journal of Hydrology*, *193*(1), 61–82. [https://doi.org/10.1016/S0022-1694\(96\)03150-2](https://doi.org/10.1016/S0022-1694(96)03150-2)
- Hope, D., Palmer, S. M., Billett, M. F., & Dawson, J. J. C. (2001). Carbon dioxide and methane evasion from a temperate peatland stream. *Limnology and Oceanography*, *46*(4), 847–857. <https://doi.org/10.4319/lo.2001.46.4.0847>
- Houze, R. A. Jr. (2012). Orographic effects on precipitating clouds. *Reviews of Geophysics*, *50*, RG1001. <https://doi.org/10.1029/2011RG000365>
- Hribljan, J. A., Cooper, D. J., Sueltenfuss, J., Wolf, E. C., Heckman, K. A., Lilleskov, E., & Chimner, R. A. (2015). Carbon storage and long-term rate of accumulation in high-altitude Andean peatlands of Bolivia. *Mires and Peat*. *15: Article 12. 14 P.*, *15*(12). Retrieved from <https://www.fs.usda.gov/treesearch/pubs/53712>
- Jalut, G., Delibrias, G., Dagnac, J., & Mardones, M. (1982). A palaeoecological approach to the last 21 000 years in the Pyrénées: The peat bog of Freychinède (alt. 1350 m, Ariège, south France). *Palaeogeography, Palaeoclimatology, Palaeoecology*.
- Jeong, J.-J., Bartsch, S., Fleckenstein, J. H., Matzner, E., Tenhunen, J. D., Lee, S. D., et al. (2012). Differential storm responses of dissolved and particulate organic carbon in a mountainous headwater stream, investigated by high-frequency, in situ optical measurements. *Journal of Geophysical Research*, *117*, G03013. <https://doi.org/10.1029/2012JG001999>
- Joosten, H., & Clarke, D. (2002). *Wise use of mires and peatlands: Background and principles including a framework for decision-making*. Jyväskylä: Greifswald: International Peat Society; International Mire Conservation Group.



- Joosten, H., Tanneberger, F., & Moen, A. (2017). *Mires and peatlands of Europe*. Stuttgart, Germany: Schweizerbart Science Publishers. Retrieved from [http://www.schweizerbart.de/publications/detail/isbn/9783510653836/Joosten\\_Tanneberger\\_Moen\\_Mires\\_and\\_peat](http://www.schweizerbart.de/publications/detail/isbn/9783510653836/Joosten_Tanneberger_Moen_Mires_and_peat)
- Kapos, V., Rhind, J., Edwards, M., Price, M. F., & Ravilious, C. (2000). Developing a map of the world's mountain forests. In M. F. Price & N. Butt (Eds.), *Forests in sustainable mountain development: a state of knowledge report for 2000. Task Force on Forests in Sustainable Mountain Development* (pp. 4–19). Wallingford: CABI. <https://doi.org/10.1079/9780851994468.0004>
- Koehler, A.-K., Murphy, K., Kiely, G., & Sottocornola, M. (2009). Seasonal variation of DOC concentration and annual loss of DOC from an Atlantic blanket bog in South Western Ireland. *Biogeochemistry*, *95*(2–3), 231–242. <https://doi.org/10.1007/s10533-009-9333-9>
- Laudon, H., Berggren, M., Ågren, A., Buffam, I., Bishop, K., Grabs, T., et al. (2011). Patterns and dynamics of dissolved organic carbon (doc) in boreal streams: The role of processes, connectivity, and scaling. *Ecosystems*, *14*(6), 880–893. <https://doi.org/10.1007/s10021-011-9452-8>
- Laudon, H., Köhler, S., & Buffam, I. (2004). Seasonal TOC export from seven boreal catchments in northern Sweden. *Aquatic Sciences*, *66*(2), 223–230. <https://doi.org/10.1007/s00027-004-0700-2>
- Le Roux, G., Hansson, S. V., & Claustres, A. (2016). Inorganic Chemistry in the mountain critical zone. *Developments in Earth Surface Processes*, *21*, 131–154. <https://doi.org/10.1016/B978-0-444-63787-1.00003-2>
- Leach, J. A., Larsson, A., Wallin, M. B., Nilsson, M. B., & Laudon, H. (2016). Twelve year interannual and seasonal variability of stream carbon export from a boreal peatland catchment. *Journal of Geophysical Research: Biogeosciences*, *121*, 1851–1866. <https://doi.org/10.1002/2016JG003357>
- Ledesma, J. L. J., Futter, M. N., Blackburn, M., Lidman, F., Grabs, T., Sponseller, R. A., et al. (2017). Towards an improved conceptualization of riparian zones in boreal forest headwaters. *Ecosystems*, 1–19. <https://doi.org/10.1007/s10021-017-0149-5>
- Leifeld, J., & Menichetti, L. (2018). The underappreciated potential of peatlands in global climate change mitigation strategies. *Nature Communications*, *9*(1), 1071. <https://doi.org/10.1038/s41467-018-03406-6>
- Marti, R., Gascoin, S., Berthier, E., de Pinel, M., Houet, T., & Laffly, D. (2016). Mapping snow depth in open alpine terrain from stereo satellite imagery. *The Cryosphere*, *10*(4), 1361–1380. <https://doi.org/10.5194/tc-10-1361-2016>
- McDonnell, J. J. (2009). Hewlett, J.D. and Hibbert, A.R. 1967: Factors affecting the response of small watersheds to precipitation in humid areas. In Sopper, W.E. and Lull, H.W., editors, *Forest hydrology*, New York: Pergamon Press, 275—90. *Progress in Physical Geography*, *33*(2), 288–293. <https://doi.org/10.1177/0309133309338118>
- Meybeck, M., Green, P., & Vörösmarty, C. (2001). A new typology for mountains and other relief classes: An application to global continental water resources and population distribution. *Mountain Research and Development*, *21*(1), 34–45.
- Moody, C. S., Worrall, F., Evans, C. D., & Jones, T. G. (2013). The rate of loss of dissolved organic carbon (DOC) through a catchment. *Journal of Hydrology*, *492*, 139–150. <https://doi.org/10.1016/j.jhydrol.2013.03.016>
- Moore, S., Evans, C. D., Page, S. E., Garnett, M. H., Jones, T. G., Freeman, C., et al. (2013). Deep instability of deforested tropical peatlands revealed by fluvial organic carbon fluxes. *Nature*, *493*(7434), 660–663. <https://doi.org/10.1038/nature11818>
- Morris, P. J., Swindles, G. T., Valdes, P. J., Ivanovic, R. F., Gregoire, L. J., Smith, M. W., et al. (2018). Global peatland initiation driven by regionally asynchronous warming. *Proceedings of the National Academy of Sciences*, *115*(19), 4851–4856. <https://doi.org/10.1073/pnas.1717838115>
- Mzobe, P., Berggren, M., Pilesjö, P., Lundin, E., Olefeldt, D., Roulet, N. T., & Persson, A. (2018). Dissolved organic carbon in streams within a subarctic catchment analysed using a GIS/remote sensing approach. *PLOS ONE*, *13*(7), e0199608. <https://doi.org/10.1371/journal.pone.0199608>
- Nilsson, M., Sagerfors, J., Buffam, I., Laudon, H., Eriksson, T., Grelle, A., et al. (2008). Contemporary carbon accumulation in a boreal oligotrophic minerogenic mire—A significant sink after accounting for all C-fluxes. *Global Change Biology*, *14*(10), 2317–2332. <https://doi.org/10.1111/j.1365-2486.2008.01654.x>
- Nogués-Bravo, D., Araújo, M. B., Errea, M. P., & Martínez-Rica, J. P. (2007). Exposure of global mountain systems to climate warming during the 21st Century. *Global Environmental Change*, *17*(3), 420–428. <https://doi.org/10.1016/j.gloenvcha.2006.11.007>
- Olefeldt, D., & Roulet, N. T. (2014). Permafrost conditions in peatlands regulate magnitude, timing, and chemical composition of catchment dissolved organic carbon export. *Global Change Biology*, *20*(10), 3122–3136. <https://doi.org/10.1111/gcb.12607>
- Pachauri, R. K., & IPCC (Eds.) (2008). *Climate change 2007: Contribution of ... to the fourth assessment report of the Intergovernmental Panel on Climate Change. 4: Synthesis report: [a report of the Intergovernmental Panel on Climate Change]*. Geneva: IPCC.
- Pawson, R. R., Evans, M. G., & Allott, T. E. H. A. (2012). Fluvial carbon flux from headwater peatland streams: Significance of particulate carbon flux. *Earth Surface Processes and Landforms*, *37*(11), 1203–1212. <https://doi.org/10.1002/esp.3257>
- Pellerin, B. A., Saraceno, J. F., Shanley, J. B., Sebestyen, S. D., Aiken, G. R., Wollheim, W. M., & Bergamaschi, B. A. (2011). Taking the pulse of snowmelt: in situ sensors reveal seasonal, event and diurnal patterns of nitrate and dissolved organic matter variability in an upland forest stream. *Biogeochemistry*, *108*(1–3), 183–198. <https://doi.org/10.1007/s10533-011-9589-8>
- Posavec, K., Giacometti, M., Materazzi, M., & Birk, S. (2017). Method and Excel VBA algorithm for modeling master recession curve using trigonometry approach. *Groundwater*, *55*(6), 891–898. <https://doi.org/10.1111/gwat.12549>
- Pullens, J. W. M., Sottocornola, M., Kiely, G., Toscano, P., & Gianelle, D. (2016). Carbon fluxes of an alpine peatland in Northern Italy. *Agricultural and Forest Meteorology*, *220*, 69–82. <https://doi.org/10.1016/j.agrformet.2016.01.012>
- Reille, M. (1990). Nouvelles recherches pollenanalytiques à Freychinède, Pyrénées ariégeoises, France. *Laboratoire de Botanique Historique et Palynologie, Novembre 1990, Pp 1-10 + Annexes*.
- Ritson, J. P. (2015). The impact of climate change and management practices on dissolved organic carbon (DOC) flux and drinking water treatment in peatland catchments.
- Rode, M., Wade, A. J., Cohen, M. J., Hensley, R. T., Bowes, M. J., Kirchner, J. W., et al. (2016). Sensors in the stream: The high-frequency wave of the present. *Environmental Science & Technology*, *50*(19), 10,297–10,307. <https://doi.org/10.1021/acs.est.6b02155>
- Rogora, M., Frate, L., Carranza, M. L., Freppaz, M., Stanisci, A., Bertani, I., et al. (2018). Assessment of climate change effects on mountain ecosystems through a cross-site analysis in the Alps and Apennines. *Science of The Total Environment*, *624*, 1429–1442. <https://doi.org/10.1016/j.scitotenv.2017.12.155>
- Rothwell, J. J., Evans, M. G., Daniels, S. M., & Allott, T. E. H. (2007). Baseflow and stormflow metal concentrations in streams draining contaminated peat moorlands in the Peak District National Park (UK). *Journal of Hydrology*, *341*(1), 90–104. <https://doi.org/10.1016/j.jhydrol.2007.05.004>
- Roulet, N. T., Lafleur, P. M., Richard, P. J. H., Moore, T. R., Humphreys, E. R., & Bubier, J. (2007). Contemporary carbon balance and late Holocene carbon accumulation in a northern peatland. *Global Change Biology*, *13*(2), 397–411. <https://doi.org/10.1111/j.1365-2486.2006.01292.x>

- Roulet, N. T., & Moore, T. R. (2006). Environmental chemistry: Browning the waters. *Nature*, *444*(7117), 283–284. <https://doi.org/10.1038/444283a>
- Ryder, E., de Eyto, E., Dillane, M., Poole, R., & Jennings, E. (2014). Identifying the role of environmental drivers in organic carbon export from a forested peat catchment. *Science of The Total Environment*, *490*, 28–36. <https://doi.org/10.1016/j.scitotenv.2014.04.091>
- Saraceno, J. F., Pellerin, B. A., Downing, B. D., Boss, E., Bachand, P. A. M., & Bergamaschi, B. A. (2009). High-frequency in situ optical measurements during a storm event: Assessing relationships between dissolved organic matter, sediment concentrations, and hydrologic processes. *Journal of Geophysical Research*, *114*, G00F09. <https://doi.org/10.1029/2009JG000989>
- Scharlemann, J. P., Tanner, E. V., Hiederer, R., & Kapos, V. (2014). Global soil carbon: understanding and managing the largest terrestrial carbon pool. *Carbon Management*, *5*(1), 81–91. <https://doi.org/10.4155/cmt.13.77>
- SOeS. (2013). Description sheets of mires areas in mainland France (p. 736). Service de l'Observation et des Statistiques. Retrieved from <https://www.statistiques.developpement-durable.gouv.fr/sites/default/files/2019-01/documents-de-travail-11-fiches-descriptives-de-massifs-a-tourbieres-de-france-metropolitaine-mars2013.pdf>
- Squeo, F. A., Warner, B. G., Aravena, R., & Espinoza, D. (2006). Bofedales: High altitude peatlands of the central Andes. *Revista Chilena de Historia Natural*, *79*(2). Retrieved from <http://www.redalyc.org/resumen.oa?id=369944278010>
- Strohmeier, S., Knorr, K.-H., Reichert, M., Frei, S., Fleckenstein, J. H., Peiffer, S., & Matzner, E. (2013). Concentrations and fluxes of dissolved organic carbon in runoff from a forested catchment: Insights from high frequency measurements. *Biogeosciences*, *10*(2), 905–916. <https://doi.org/10.5194/bg-10-905-2013>
- Szczypta, C., Gascoin, S., Houet, T., Hagolle, O., Dejoux, J.-F., Vigneau, C., & Fanise, P. (2015). Impact of climate and land cover changes on snow cover in a small Pyrenean catchment. *Journal of Hydrology*, *521*, 84–99. <https://doi.org/10.1016/j.jhydrol.2014.11.060>
- Tang, J., Yurova, A. Y., Schurgers, G., Miller, P. A., Olin, S., Smith, B., et al. (2018). Drivers of dissolved organic carbon export in a subarctic catchment: Importance of microbial decomposition, sorption-desorption, peatland and lateral flow. *Science of The Total Environment*, *622–623*, 260–274. <https://doi.org/10.1016/j.scitotenv.2017.11.252>
- Tang, R., Clark, J. M., Bond, T., Graham, N., Hughes, D., & Freeman, C. (2013). Assessment of potential climate change impacts on peatland dissolved organic carbon release and drinking water treatment from laboratory experiments. *ResearchGate*, *173*, 270–277. <https://doi.org/10.1016/j.envpol.2012.09.022>
- Ternet, Y., Colchen, M., Debroas, E., Azambre, B., Debon, F., Bouchez, J., et al. (1997). Notice explicative carte géol. France (1/50 000), feuille Aulus-les-Bains (1086). BRGM Editions, Orléans.
- Tetzlaff, D., Birkel, C., Dick, J., Geris, J., & Soulsby, C. (2014). Storage dynamics in hydrogeological units control hillslope connectivity, runoff generation, and the evolution of catchment transit time distributions. *Water Resources Research*, *50*, 969–985. <https://doi.org/10.1002/2013WR014147>
- Tipping, E., Smith, E. J., Lawlor, A. J., Hughes, S., & Stevens, P. A. (2003). Predicting the release of metals from ombrotrophic peat due to drought-induced acidification. *Environmental Pollution*, *123*(2), 239–253. [https://doi.org/10.1016/S0269-7491\(02\)00375-5](https://doi.org/10.1016/S0269-7491(02)00375-5)
- Tunaley, C., Tetzlaff, D., Lessels, J., & Soulsby, C. (2016). Linking high-frequency DOC dynamics to the age of connected water sources. *Water Resources Research*, *52*, 5232–5247. <https://doi.org/10.1002/2015WR018419>
- Tunaley, C., Tetzlaff, D., Wang, H., & Soulsby, C. (2018). Spatio-temporal diel DOC cycles in a wet, low energy, northern catchment: Highlighting and questioning the sub-daily rhythms of catchment functioning. *Journal of Hydrology*, *563*, 962–974. <https://doi.org/10.1016/j.jhydrol.2018.06.056>
- Vidal, J.-P., Martin, E., Franchistéguy, L., Baillon, M., & Soubeyrou, J.-M. (2010). A 50-year high-resolution atmospheric reanalysis over France with the Safran system. *International Journal of Climatology*, *30*(11), 1627–1644. <https://doi.org/10.1002/joc.2003>
- Viviroli, D., Dürr, H. H., Messerli, B., Meybeck, M., & Weingartner, R. (2007). Mountains of the world, water towers for humanity: Typology, mapping, and global significance. *Water Resources Research*, *43*, W07447. <https://doi.org/10.1029/2006WR005653>
- Walling, D. E., & Webb, B. W. (1985). Estimating the discharge of contaminants to coastal waters by rivers: Some cautionary comments. *Marine Pollution Bulletin*, *16*(12), 488–492. [https://doi.org/10.1016/0025-326X\(85\)90382-0](https://doi.org/10.1016/0025-326X(85)90382-0)
- Watras, C. J., Hanson, P. C., Stacy, T. L., Morrison, K. M., Mather, J., Hu, Y.-H., & Milewski, P. (2011). A temperature compensation method for CDOM fluorescence sensors in freshwater. *Limnology and Oceanography: Methods*, *9*(7), 296–301. <https://doi.org/10.4319/lom.2011.9.296>
- Webb, J. R., Santos, I. R., Maher, D. T., & Finlay, K. (2018). The importance of aquatic carbon fluxes in net ecosystem carbon budgets: A catchment-scale review. *Ecosystems*, *22*(3), 508–527. <https://doi.org/10.1007/s10021-018-0284-7>
- Worrall, F., Reed, M., Warburton, J., & Burt, T. (2003). Carbon budget for a British upland peat catchment. *Science of The Total Environment*, *312*(1), 133–146. [https://doi.org/10.1016/S0048-9697\(03\)00226-2](https://doi.org/10.1016/S0048-9697(03)00226-2)
- Yu, Z., Loisel, J., Brosseau, D. P., Beilman, D. W., & Hunt, S. J. (2010). Global peatland dynamics since the Last Glacial Maximum: Global peatlands since the LGM. *Geophysical Research Letters*, *37*, L13402. <https://doi.org/10.1029/2010GL043584>
- Zemp, M., Haeberli, W., Hoelzle, M., & Paul, F. (2006). Alpine glaciers to disappear within decades? *Geophysical Research Letters*, *33*, L13504. <https://doi.org/10.1029/2006GL026319>